Explore Adsorption Compression Using Computational and Experimental Methods

By

Yutian Qian

A thesis submitted to Johns Hopkins University in conformity with the requirements for the degree of Master of Science in Engineering

Baltimore, Maryland

May 2019

Abstract

Adsorption is the phenomenon of liquid, gas, or sometimes solid molecules adhering to a surface of solid. It is crucial and widely applied in chemical industries, such as heterogeneous catalysis and many other fields. Adsorption compression, a phenomenon observed from both experimental and computational results, is introduced and studied recently to see how adsorbate-adsorbate repulsive forces can affect the adsorption on the surface. This novel perspective gives insights about adsorption under various circumstances.

This thesis includes two parts of adsorption compression related study: the first part is to use computational methods, namely the Monte Carlo (MC) simulation, to calculate the adsorbate distribution in a confined space in comparison to the surface of adsorbent. Prior literature about MC simulations will be discussed to elaborate the work. The second part, which is the focus of this thesis study, involves using AutoChem II 2920 Chemisorption Analyzer paired with OmniStar GSD320 Mass Spectrometer (MS) to conduct Temperature-Programmed Desorption (TPD) experiments of carbon monoxide (CO) on zeolite H-ZSM-5 at 35ºC. The concentration of CO used in the experiment ranges from 3.5 part per million (ppm) to 10%. The practice of tracking the gas component during the TPD analysis with MS is not employed in many studies. And with the MS data, the CO desorption peak provides useful information to describe the adsorption compression. Both computational and experimental methods validate that the adsorption compression phenomenon occurs on the adsorbent surface. The evidence of adsorption compression may help us enhance catalysts performance in reducing toxic NO_x exhaust gas from vehicles and other related catalytic processes.

Thesis Committee:

Dr. Marc D. Donohue, Professor of Chemical and Biomolecular Engineering

Dr. Gregory Aranovich, Principle Research Scientist of Chemical and Biomolecular Engineering

Table of Contents

Acknowledgement

I would like to thank my advisor Dr. Marc Donohue and co-advisor Dr. Gregory Aranovich for their instructions and guidance not only on my research work, but also on my future. In every weekly discussion, I adsorbed new knowledge from them. I really appreciate their time and energy spent with me to conduct my research project over the past two years. I am so grateful to their kindness and patience when I struggled in research. This thesis work could not be finished without their assistance in teaching me the theoretical background, constructing the computational modeling, designing the experiment, and raising up insightful ideas of how adsorption compression would possibly develop in the catalytic system.

I would also like to express my gratitude to the Post-docs, Pengfei and Peikun, visiting Doctorate student Junlei and other group members from Dr. Chao Wang's lab for their help in showing me the basics of building up a lab from scratch.

I would like to thank my friends, Pingfan and Nianchao, for bringing up so much fun outside of the research work. I would like to thank my parents, Hong and Ping, for their support and encouragement throughout my master study and whole life. Lastly, I would like to dedicate this thesis to my grandmother Xiaoyuan. You made me become the person who I am, everything would be different without your presence in my life, and I would always remember what you have taught me.

List of Tables

List of Figures

1. Introduction

Adsorption and Its Categorization

Adsorption, according to International Union of Pure and Applied Chemistry (IUPAC) Gold Book[1], is "an increase in the concentration of a dissolved substance at the interface of a condensed and a liquid phase due to the operation of surface forces." Unlike absorption where molecules are dissolved by or permeate into a liquid or solid bulk phase, adsorption is the adhesion of gas, liquid, or solid molecules to a surface. The condensed bulk phase at the adsorbing surface is defined as adsorbent whereas the adsorbed molecules on the surface are adsorbates[1-2]. Figure 1 illustrates the different mechanisms between adsorption on a liquid-solid interface and absorption of a gas-liquid system where the former one occurs at the interface and the latter is a bulk phenomenon involving the whole volume of the material[3]. Figure 2 depicts the process of adsorption of adsorbate onto a flat, homogeneous adsorbent surface. It also shows the interaction between the adsorbates and adsorbents. Both adsorption and absorption are specific cases of sorption, a physical and chemical process by which one substance is attracted to another[4].

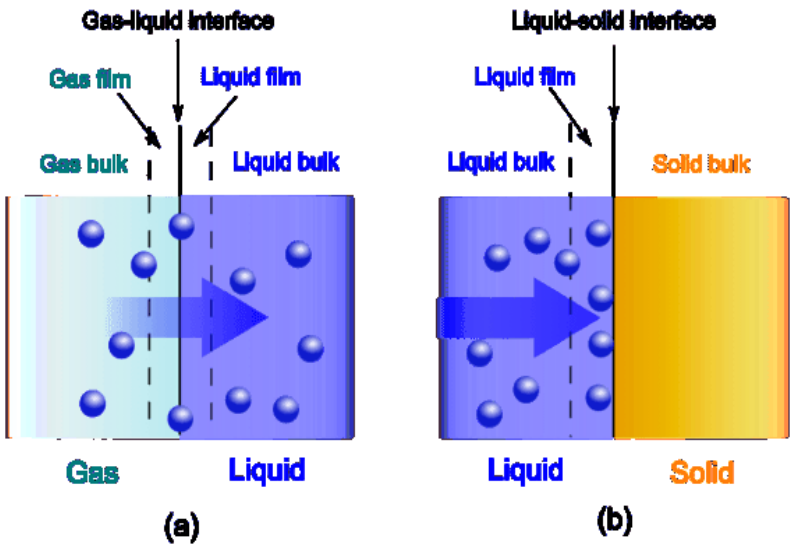

Figure 1: Gas-liquid absorption (a) and liquid-solid adsorption (b) mechanism

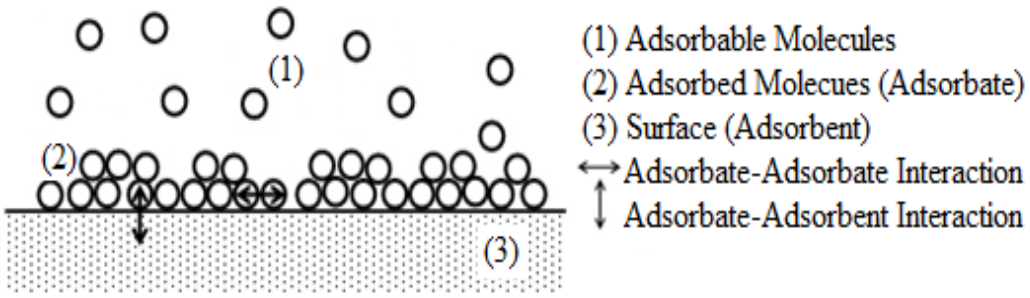

Figure 2: Adsorption of adsorbate onto a flat, homogeneous adsorbent surface[5]

Adsorption can be divided into two different types: physisorption and chemisorption. In physisorption, the fundamental interacting force between the adsorbate and the adsorbent is van der Waal force. The term van der Waal adsorption is synonymous with physisorption. Because the van der Waal interactions are relatively weak, the heat of adsorption for physisorption is around 20~40 $kJ \cdot mol^{-1}$. Physisorption usually is a reversible process. It is favored at low temperature and can invovle multi-layer adsorption. On the other hand, chemisorption involves the formation of new chemical bonds and therefore requires the transfer of the electrons between the adsorbate and the adsorbent. The strong chemical bonding makes the heat of adsorption much higher, ranging from 40~400 $kJ \cdot mol^{-1}$. Chemisorption often requires an activation energy in its elementary step, and new compounds are created on the surface. Desorption of the original species may not be recovered so chemisorption is irreversible. Chemisorption favors high temperature conditions and it only form a mono-layer of adsorbate or less on top of the interface[6]. The major differences between physisorption and chemisorption are shown in Table 1.

Table 1: Major differences between chemisorption and physisorption

	Chemisorption	**Physisorption**
Interaction	Chemical bonding	Intermolecular forces
Heat of Adsorption	40~400 kJ·mol^{-1}	20~40 kJ·mol^{-1}
Temperature Preference	High temperature	Low temperature
Reversibility	Irreversible	Reversible
Number of Layers	Mono-layer	Multi-layer
Example	Self-Assembled-Monolayers	Gas molecules on metal surfaces

Adsorption Isotherm

The adsorption isotherm is used to study the process of adsorption behavior as it shows the relation between the quantity of adsorbed adsorbate and its composition in the bulk phase under equilibrium conditions at constant temperature[7]. It is usually plotted with the normalized units such as specific adsorbed amount of adsorbate (moles per unit mass) against adsorbate's relative pressure (equilibrium pressure over its saturation pressure) at a given temperature[8]. This practice allows the comparison of isotherms obtained from different materials.

Figure 3 shows six major types of adsorption isotherms classified by IUPAC. The first five types of classification were originally proposed in 1940 by S. Brunauer, Deming, Deming, and Teller, so sometimes they are also referred as the BDDT or just the Brunauer classifications[9]. The last Type IV has been observed more recently and is included in 1985 IUPAC classification. In this section, Type I and Type II isotherm are introduced briefly as they are encountered more often compared to others.

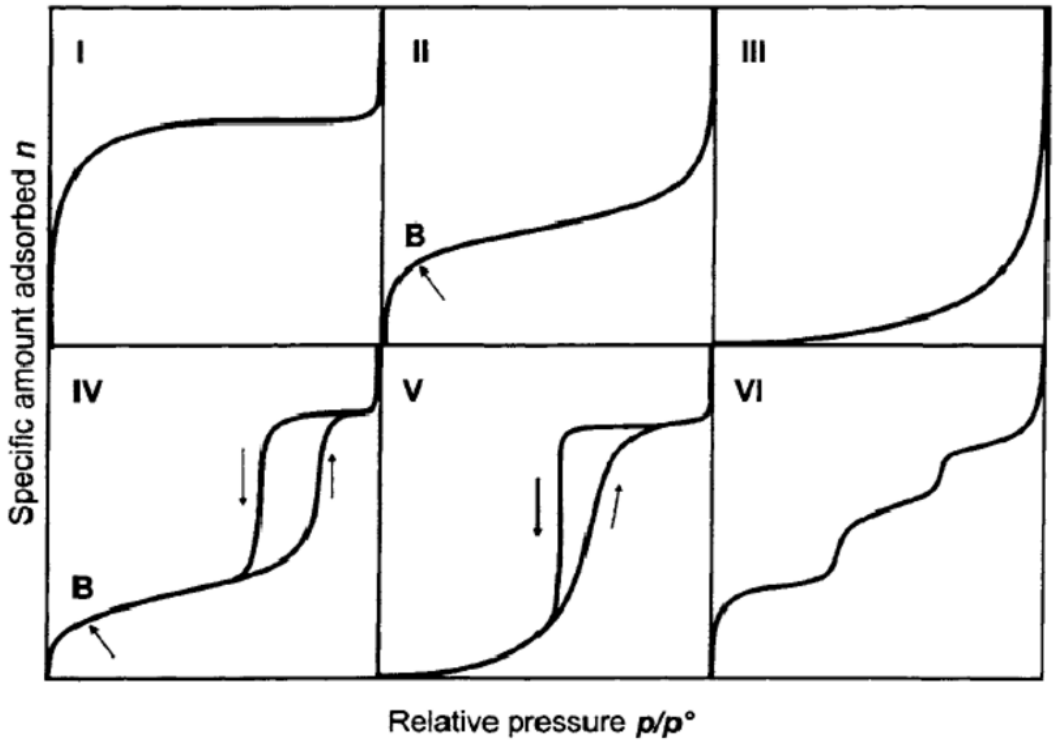

Figure 3: Six main types of adsorption isotherm based on IUPAC classification

Type I isotherm, in its most characteristic form, is concave to the relative pressure, the y-axis. At low relative pressure, the isotherm rises sharply and reaches a plateau, which is the limiting value as the relative pressure approaches to 1. This type of isotherms is seen in microporous materials having mainly narrow micropores (of width less than 2 nm) and relatively small external surfaces, such as molecular sieve zeolites[10-11]. Type I isotherms also are referred as Langmuir-like isotherm as the curve follows the Langmuir isotherm equation:

$$\theta_A = \frac{v}{v_m} = \frac{K_{eq}^A p_A}{1 + K_{eq}^A p_A} \quad (1)$$

where θ_A is the fractional coverage of the adsorbent A, v is the volume of adsorbed layer, v_m is the total volume capacity of the monolayer, p_A represents the adsorbate's partial pressure, K_{eq}^A is the equilibrium constant for the ad/desorption system[12]. Langmuir's isotherm has many

assumptions, such as homogeneous surface, monolayer coverage, no interactions between adsorbate molecules, that make it the simplest case of the adsorption isotherm[13].

Type II isotherm are seen for adsorption of most gases on nonporous or mesoporous (pore size > 50 nm) adsorbent. The isotherm is first concave to the y-axis, then turns linear, and finally becomes convex to the y-axis. This indicates the formation of multi-layer adsorbate coverage on the surface of the adsorbent. In Figure 3, point B in Type II isotherm curve, the beginning of the middle quasilinear section, is usually considered as the completion of the monolayer adsorption and the beginning of the multilayer adsorption. As the relative pressure approaches 1, the adsorbed layer thickness appears to increase without limit, which indicates the layer becomes a bulk liquid or solid[9-10]. The BET equation, developed by Brunauer, Emmett, and Teller, is used to determine adsorption of gases in multilayer surface, and it can represent the Type II adsorption isotherm. The original BET equation is:

$$\frac{p}{v(p_0 - p)} = \frac{1}{v_m c} + \frac{c-1}{v_m c}\frac{p_A}{p_0} \quad (2)$$

where p_A and p_0 are the equilibrium and the saturation pressure of adsorbate respectively, v and v_m, similar to their definition in Eqn. (1), are the volume of adsorbed adsorbate and the total volume capacity of the monolayer, c is the BET constant. By mathematical transformation of putting v/v_m as θ_A, p_A/p_0 as x_A, Eqn. (3) can be obtained and used to describe Type II adsorption isotherm:

$$\theta_A = \frac{cx_A}{(1 - x_A)(1 - x_A + cx_A)} \quad (3)$$

Type III, IV, V, and VI adsorption isotherm are also observed in adsorption processes but are relatively rare to see. The six types of adsorption isotherm are necessarily a simplification since more complex isotherms are observed experimentally. The classification is also only applicable to

the adsorption of single-component gas within its condensable range of temperature. Nonetheless it is very useful for the characterization of porous materials[8].

Adsorption Compression

Most of the classical models that are used to study adsorption assume or derive that the adsorbed molecules interact with each other through attractive forces on the interface. However, the phenomenon of compression of molecules in adsorbed phases has been observed by theoretical predictions[14-15], molecular simulations[16-17], and experiments[18-21], yet this phenomenon has not been systematically formulated and discussed earlier until the published literature of Aranovich and Donohue[22]. Adsorption compression occurs when the strong field of adsorbent pulls adsorbates to the surface and creates a density higher than in a normal liquid. At this state the adsorbate molecules repel each other until there exists a balance between the free energy loss due to strong surface attraction and the free energy gain due to the repulsion[23].

Two different cases of adsorption compression are shown in Figure 4 and 5. Figure 4 illustrates two molecules on the surface where two active sites can be occupied with different distances between them. It can be interpreted as a two-site model. When the distance between the active sites is large, adsorbate molecules can sit on the sites independently (a). As the active sites are closer, both sites can still be occupied but the adsorbate molecules repel each other (b). This case will only be possible if the attraction between the adsorbate and active sites is stronger than the repulsion between the neighboring adsorbate molecules and it is the simplest case of the adsorption compression. At very small distance between active sites (c), the adsorption compression effect disappears as one adsorbed molecule is blocking the neighboring active site, preventing the other adsorbate molecule from adsorbing. This is caused by a larger repulsion between neighbors exceeding the attraction of adsorbate molecules to the active sites[22].

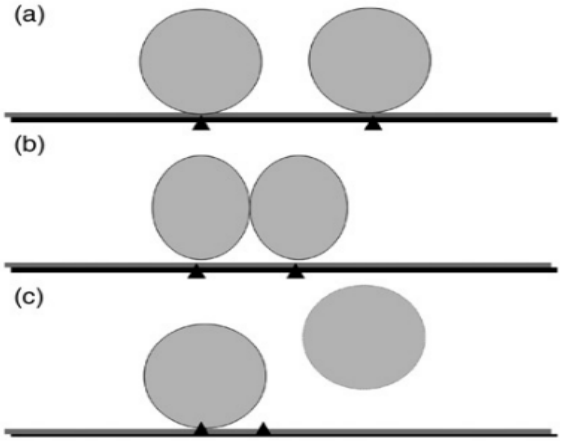

Figure 4: Adsorption compression on two adjacent active sites

Similarly, Figure 5 shows adsorbate molecules in a trough on a surface with (a) low density and (b) high density. This is a representation of adsorption compression in a real system corresponding to the one-dimensional box[22].

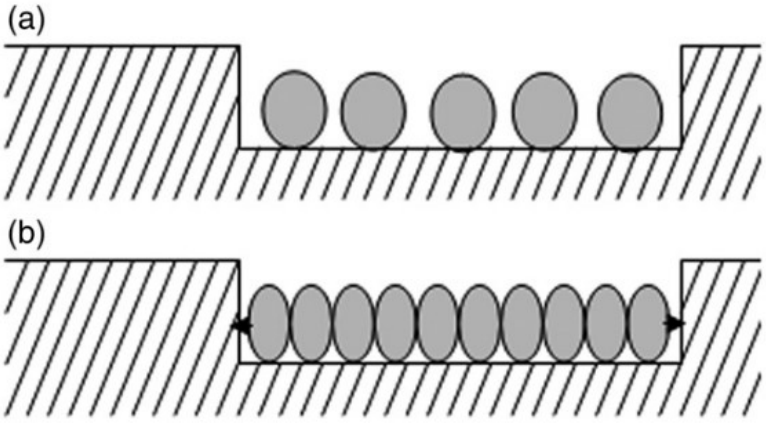

Figure 5: Molecules in a trough on a surface with (a) low and (b) high density

The adsorbate-adsorbate interactions can be described using the Lennard-Jones (L-J) potential function, a function of potential energy (φ) between two molecules with respect to the distance (d) between them. The L-J potential function is written as:

$$\varphi(d) = 4\varepsilon_0 \cdot \left[\left(\frac{d}{\sigma}\right)^{-12} - \left(\frac{d}{\sigma}\right)^{-6}\right] \quad (4)$$

where ε_0 is the depth of the potential well and is positive, the region surrounding a local minimum of potential energy, d is the distance between particles, and σ the finite distance at which the inter-particle potential is zero, i.e. the diameter or the Van der Waal radius of the molecule [24]. The plot of L-J potential function and its force derivative is shown in Figure 6.

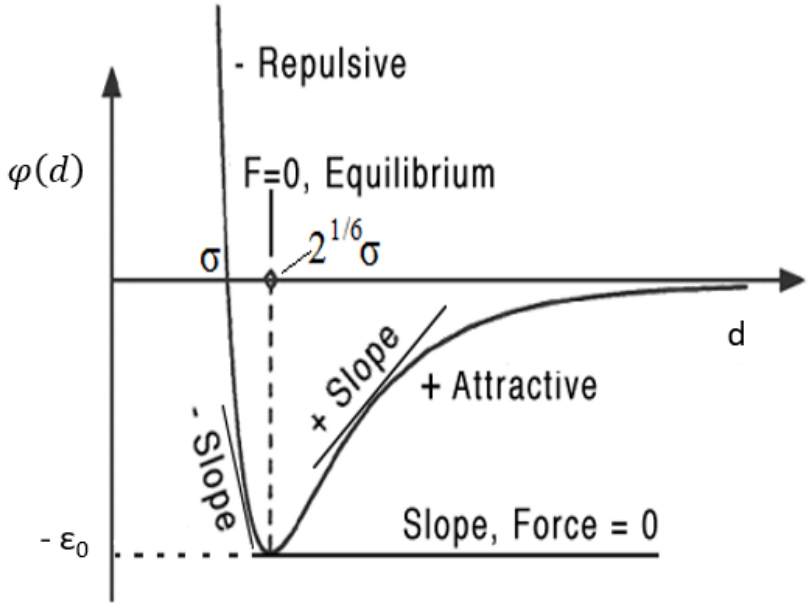

Figure 6: Lennard-Jones potential function and its force derivative

when two molecules are far away from each other (d is large), the potential is negative and the slope of the potential function, which is the interacting forces between two molecules is positive, indicating an attractive force. As two molecules gradually approach to each other, at d= $2^{1/6}\sigma$, the potential reaches its minimum at the value of the potential well $-\varepsilon_0$. The net force experienced by two molecules is zero at this point. When $d < 2^{1/6}\sigma$, the molecules have repulsive forces between them as the slope of the potential turns to negative. During this stage, adsorption compression would happen. The potential becomes zero when $d = \sigma$.

Ono-Kondo Equation & Coordinate

One method to determine the occurrence of adsorption compression from an adsorption isotherm is to plot the adsorption isotherm in the Ono-Kondo coordinates. By doing this, the slope of the curve in Ono-Kondo coordinate indicate whether the intermolecular forces are repulsive or attractive.

The derivation of Ono-Kondo equation and coordinates are shown as follows[23,25-26]. Consider taking an adsorbate molecule from an adsorption site on the surface and putting it into an empty space between molecules in the bulk. This is equivalent to the exchange of a molecule with a vacancy as:

$$M_a + V = V_a + M \text{ [5]}$$

where M is the adsorbate molecule and V is the empty space in the bulk. The subscript a denotes that the adsorbate molecule and empty space is in the adsorbed layer. At equilibrium, the Gibbs free energy ΔG equals to zero. It is composed of both enthalpy and entropy changes as:

$$\Delta G = \Delta H - T\Delta S = 0 \text{ [6]}$$

where ΔH is the enthalpy term, T is absolute temperature in Kelvin, ΔS is the entropy change term. With mean-field lattice approximation, the value of ΔS can be represented in the form of

$$\Delta S = k \ln \frac{x_a(1 - x_b)}{(1 - x_a) \cdot x_b} \text{ [7]}$$

where k is the Boltzmann's constant, $x_a$is the probability that the certain site in the adsorbed phase is occupied, and x_b is the density of adsorbate in bulk. The enthalpy change term, in general case with no geometric specification, is expressed as:

$$\Delta H = k_0\varepsilon_s + k_1\varepsilon_a x_a - k_2\varepsilon_b x_b \text{ [8]}$$

where k_0, k_1, k_2 are the coordination numbers, $\varepsilon_s, \varepsilon_a, \varepsilon_b$are the interaction energy between the adsorbate-adsorbent, adsorbate-adsorbate in adsorbed layer, adsorbate-adsorbate in the bulk

respectively. Combine Eqn. [6], [7], and [8] together, the relation between x_a and x_b can be obtained as:

$$x_a = \frac{x_b}{x_b + (1 - x_b)\exp(\frac{k_0\varepsilon_s + k_1\varepsilon_a x_a - k_2\varepsilon_b x_b}{kT})} \quad [9]$$

The term $-k_2\varepsilon_b x_b$ normally is very small because x_b typically is around 10^{-3} for vapors, therefore it can be ignored in most adsorption systems. For the remaining interaction energy term, $k_0\varepsilon_s$ and $k_1\varepsilon_a x_a$, $k_0\varepsilon_s$ is dominant. Therefore, after mathematical manipulation, Eqn. [9] can be written as:

$$\ln\frac{x_a(1 - x_b)}{H(1 - x_a)x_b} = \frac{-k_1\varepsilon_a x_a + k_2\varepsilon_b x_b}{kT} \quad [10]$$

where Henry's constant, $H = \exp(-\frac{k_0\varepsilon_s}{kT})$. This equation can be used to find the useful information about the second-order contribution $k_1\varepsilon_a x_a$ of interactions in the adsorbed phase. Simplify by denoting Y as the left-hand side in Eqn. [10], Eqn. [11] is obtained and it reflects the characteristics of interacting forces between adsorbed layer in the slope term $-k_1(\frac{\varepsilon_a}{kT})$ if we plot Y/x_b against x_a/x_b. Since the coordination number k_1 and k_2 are positive values, a negative slope $-k_1(\frac{\varepsilon_a}{kT})$ indicates positive interaction energy of ε_a, and from L-J potential function plot, it lies the potential energies for interacting molecules in adsorbed layer. Vice versa, a positive slope indicates attractive energies between adsorbate molecules in the adsorbed layer.

$$Y/x_b = -k_1\left(\frac{\varepsilon_a}{kT}\right)\left(\frac{x_a}{x_b}\right) + \frac{k_2\varepsilon_b}{kT} \quad [11]$$

Figure 7 illustrates the adsorption isotherm calculated from Eqn. [9] with k_0, k_1, k_2 equals to 5,1, and 6 respectively. In Figure 7, the two isotherms have the same parameter of $\varepsilon_s/kT = -4.5, \varepsilon_b/kT = -0.6$, and different ε_a/kT value as the ε_a/kT of lower curve is +0.6 (repulsive) and -0.6 for the upper curve (attractions). Even though the two isotherms have the same Henry's constant at low density region, they are significantly different at medium and high densities.

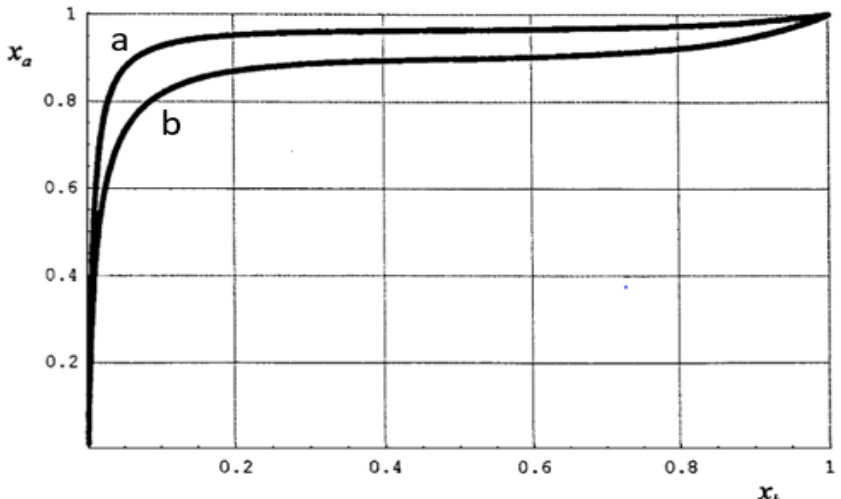

Figure 7: Dependence of x_a on x_b at ε_s /kT =−4.5, ε_b /kT =−0.6, and different ε_a /kT: −0.6 (a), +0.6 (b)

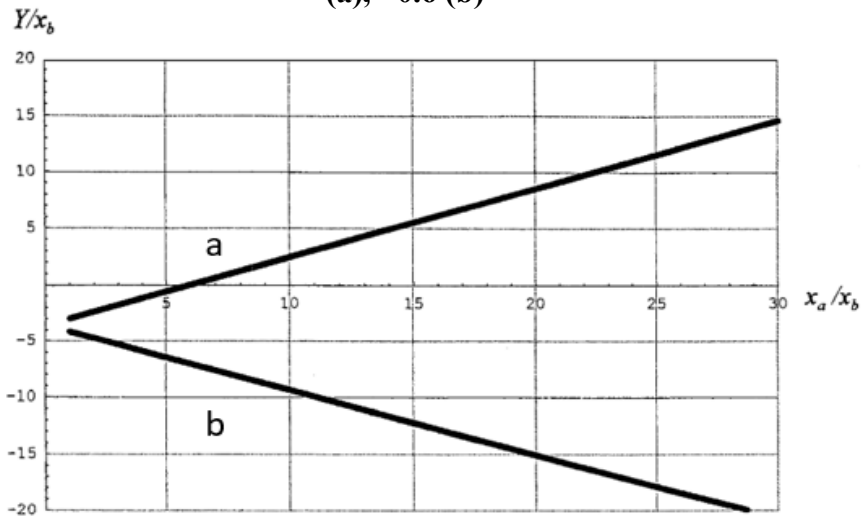

Figure 8: Adsorption isotherm of Figure 7 in coordinate of Eqn.[6] with ε_a /kT: −0.6 (a), +0.6 (b) (Ono-Kondo Coordinate)

Figure 8 shows the adsorption isotherms given in Figure 7 in coordinates of Eqn. [11]. The upper curve (a) with a positive slope represents the upper isotherm (a) in Figure 7 while the lower curve (b) with a negative slope represents the lower isotherm (b) in Figure 7. It is hard to distinguish the difference in molecular interaction based on the two isotherms shown on Figure 7, however, the signs of the slopes in Figure 8 clearly show the difference in attractive or repulsive energies when positive slope indicates attractive energies and negative slope indicates repulsive

energies[23]. The Ono-Kondo coordinate in Figure 8 gives useful information about the nature of intermolecular forces with the given adsorption isotherm.

2. Computational Study of Adsorption Compression with Monte Carlo (MC) Methods

Computational methods, namely the Monte Carlo (MC) simulation, will be discussed in this section of the work. Prior literature on Grand Canonical Monte Carlo (GCMC) simulations of molecules on a flat surface shows useful insights into the mechanism and effects of adsorption compression. The theoretical background of Markov Chain Monte Carlo (MCMC), the Metropolis-Hastings (M-H) algorithm and other techniques employed within the 2-D Canonical Ensemble simulation will be introduced as well.

Theoretical Background of Markov Chain Monte Carlo (MCMC) Simulation

Originating in 1940s, the Monte Carlo method is a computer simulation which is based on repeated random sampling, i.e., using random numbers in scientific sampling. It uses random numbers to solve problems with a large number of coupled degrees of freedom that are difficult to solve using other simple computational methods. The Monte Carlo simulation can be applied to a wide range of scientific areas, such as the molecular modeling of an adsorption system where the configurations are generated using equilibrium probability, π, based on different statistical mechanical ensembles[27]. Figure 9 illustrates the steps of conducting a Monte Carlo simulation.

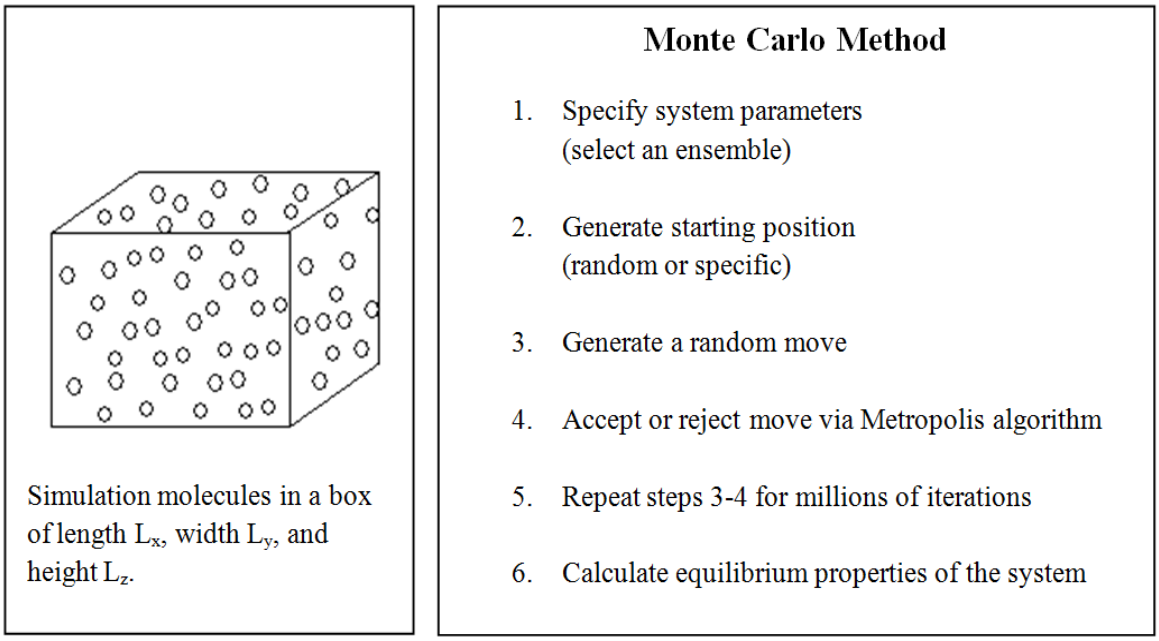

Figure 9: Basic steps of Monte Carlo simulations

The first step in Monte Carlo simulation is to select the system parameters, i.e., select an ensemble. The most common ensemble used in Monte Carlo simulation is the grand canonical ensemble which holds chemical potential, μ, absolute temperature, T, and system volume, V as constant. Sometimes the canonical ensemble which hold number of particles, N, absolute temperature, T, and system volume, V, as constant is also used in the simulation. Generating a starting configuration of the system is the next step. The initial configuration could be generated either randomly or with a specific selection. After generating the initial configuration, a random move or change of the current configuration takes place. It is a perturbation of the original one, and it is carried out with full randomness. The system will not always move on to the new configuration after the perturbation. A specific standard is used to accept or reject the random move from the current state. All of the steps mentioned above then will be iterated for a large number of times which will eventually lead to the desired equilibrium configuration expected or specified. During

the repetition, the interested properties can be collected for every thousand moves so that an average value could be generated.

Markov Chain Monte Carlo (MCMC) is one of the popular sampling methods under the category of Monte Carlo simulation. It implements the Markov Chain property into the Monte Carlo simulation so that every new configuration generated by the random walk will only base on the previous configuration and has nothing to do with all the past configurations, and the number of iterations into the simulation has no influences in generating the new configurations[28].

The Metropolis-Hastings algorithm, proposed by Metropolis and developed by Hastings, is a Markov chain Monte Carlo method for obtaining a sequence of random samples from a probability distribution from which direct sampling is difficult. Metropolis algorithm is a special case of the Metropolis-Hastings algorithm where the proposal function is symmetric. Metropolis algorithm is reflected in the step of accepting or rejecting the new configuration by creating an acceptance ratio α. By comparing the acceptance ratio α with a random number μ, it is decided whether to accept the new configuration generated from random walk or keep the old one[29,30]. An explanation of the Metropolis algorithm is shown as follows:

Suppose the current configuration has a probability distribution for the current configuration is $\pi(old)$, and the probability distribution after perturbation is $\pi(new)$. There exists an arbitrary probability density $g(o|n)$ which is the probability of changing from distribution $\pi(o)$ to $\pi(n)$. Similarly, the probability density $g(n|o)$ is the probability of changing from configuration $\pi(n)$ to $\pi(o)$. The ratio of probabilities of going from the current configuration to the new one after random walk is calculated as $\alpha = \min\{1, \frac{\pi(n)g(n|o)}{\pi(o)g(o|n)}\}$. In M-H algorithm, the probability density g has to be symmetric, meaning $g(o|n) = g(n|o)$. Therefore, $\alpha = \min\{1, \frac{\pi(n)}{\pi(o)}\}$, which is the minimum value between 1 and $\frac{\pi(n)}{\pi(o)}$. After generating the acceptance

ratio α, another uniform random number μ is created in the interval between 0 and 1. If $\mu \leq \alpha$, the transition from configuration of $\pi(o)$ to configuration of $\pi(n)$ is accepted. Otherwise, as $\mu > \alpha$, the configuration of the system will remain the same.

The 2-D MCMC canonical ensemble simulation is trying to minimize the potential energy of the 2-D lattice system while keeping the number of molecules constant. For the current work, each molecule will only occupy for one lattice spot, and only the closest neighboring molecules will be considered to have a significant interaction with the molecule in the center. In a 2-D canonical ensemble simulation, after generating an initial configuration in the lattice representing the flat surface, new configurations are generated by random walk only depending on the previous configuration. Also, the probability distribution π in a 2-D canonical ensemble simulation could be interpreted as the total potential energy of the system. Thus, the acceptance ratio in M-H algorithm is trying to compare the total potential energy between the two configurations: if the total energy of the new configuration is smaller than the old one, i.e. $\frac{\pi(n)}{\pi(o)}$ <1, it has a probability for the system to move on to the new configuration based on the value of random generated number μ. On the other hand, if the total potential energy of the new configuration is larger, i.e. $\frac{\pi(n)}{\pi(o)}$ >1, the acceptance ratio becomes 1 and there is still a probability that the transition will be accepted. This simulation provides an equilibrium configuration with the minimum total potential energy for given number of molecules adsorbed on a pre-set lattice. The distribution density data obtained after many iterations will be useful in future exploration of the Checkerboard theory presented in Shao-Hsuan Lin's thesis work.

Grand Canonical Monte Carlo (GCMC) Studies in Prior Literature

As mentioned in the previous section, Grand Canonical (GC) ensemble holds chemical potential, μ, absolute temperature, T, and system volume, V as constant. Thus, it is also named as

the μVT ensemble. It is particularly useful in the gas-solid adsorption system simulation since the chemical potential, μ, is an independent variable in the GC ensemble, which reflects the conditions in real situations. It is also a very effective method to study the gas-solid system such that the transition from one configuration to another can be achieved rapidly with short translational movement of molecules. Abaza et al.[31] uses GCMC method to simulate the adsorption process of gas molecules on a homogeneous flat surface. The study provides useful information and data to prove the occurrence of adsorption compression considering the number of molecules adsorbed in the surface layer and the interaction between the adsorbed molecules. The simulation details will not be described here, but it could be tracked in Abaza's thesis work and her research paper[31].

Figure 10 shows the adsorption isotherm for a system with an isosteric heat of adsorption at ε/kT =-1.0 and ε_s/kT values varying from -3, weakly adsorbing case, to -30 strongly adsorbing case. The ε and ε_s values represent parametesr in the Lennard-Jones potential function for adsorbate-adsorbate and adsorbate-adsorbent interactions respectively. Notice that the y-axis in Figure 10 and subsequent figures is normalized density such that the value turns to unity when the L-J potential function for adsorbate-adsorbate interaction is at minimum, i.e., $d = 2^{1/6}\sigma$. This practice helps differentiate different cases of adsorption as the normalized density is smaller, equal, or larger than unity. When normalized density is smaller than unity, it means the active site (pores) on the surface is not fully occupied. A unity normalized density indicates a completely covered adsorbed layer on the surface. While a normalized density greater than unity represents the first adsorbed layer is being compressed and tends to form a second adsorbed layer. For all range of ε_s/kT values, the adsorption isotherm rises rapidly to unity and then flattens to create a plateau before rising rapidly again. For the rest of analysis, the isotherm and simulation results for adsorbate-adsorbent interaction $\varepsilon_s/kT = -30$ will be the focus as it reflects the greatest

interaction between the adsorbate and the adsorbent, which is used to compensate the energy gain due to the repulsion in adsorbate layers to reach equilibrium.

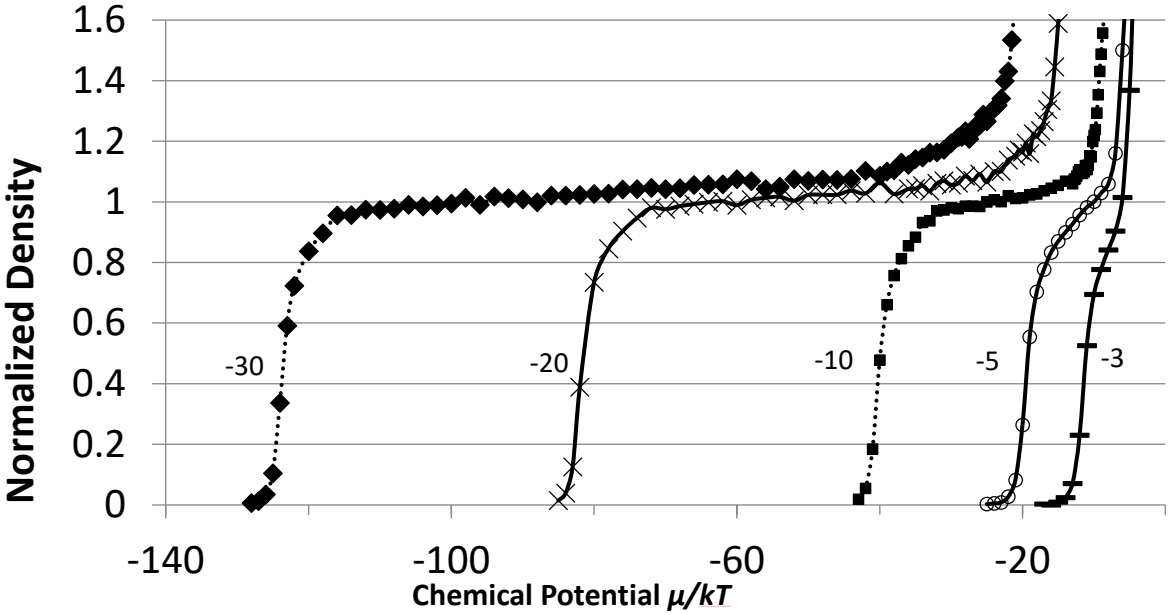

Figure 10: Adsorption Isotherm of Molecules on a Flat Surface with ε /kT= -1 and variable εs /kT: -3, -5, -10, -20, and -30

The snapshot of the packing of adsorbed molecules on the surface with different chemical potentials is shown in Figure 11 and Figure 12. Initially there are n=254 adsorbed molecules in the first adsorbed layer within a 16×16 space. There are also not many overlapping of molecules in the starting configuration. As the chemical potential increases, more adsorbed molecules have been added to the system, the packing of the molecules becomes tighter. Interestingly, more molecules (over n=256) are contained in the 16×16 adsorption surface compared to the available slots. Two possible explanations could be drawn from the phenomenon: one is that there are a second adsorbed layer formed so that more molecules are added to the system; second explanation is the adsorption compression takes place in the first adsorbed layer, causing molecules closely packed together to make space for additional molecules.

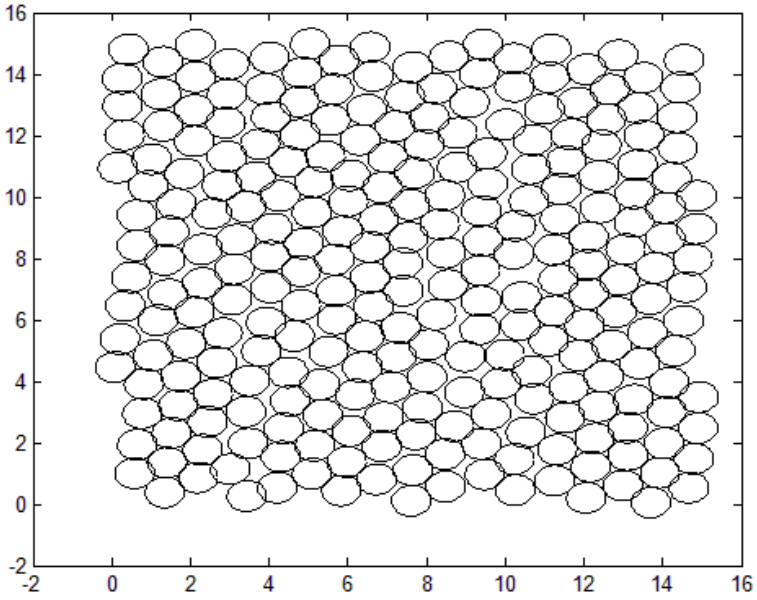

Figure 11: 2-Dimensional snapshot of the adsorbed molecules on the flat surface for ε/kT = -1.0, ε_s /kT = -30 and μ/kT =-112. N = 254, ρ=0.98

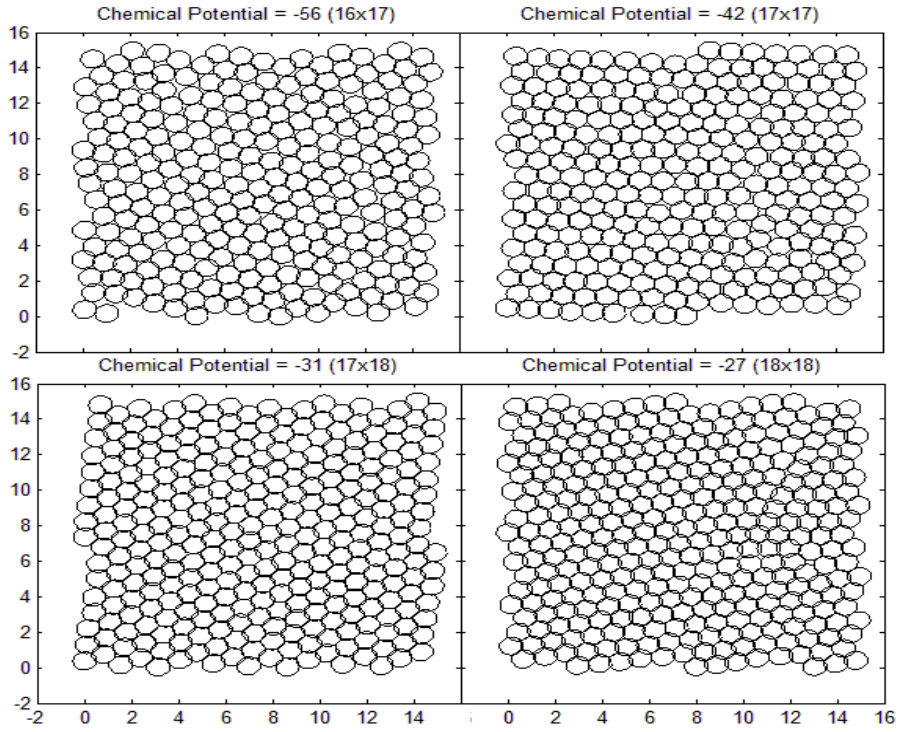

Figure 12: Snapshot of the adsorbed molecules on the flat surface for ε/kT = -1.0, ε_s /kT = -30 and various μ/kT

An analysis of combining simulation data as a function of distance from the surface has been conducted to check if there is a second adsorbed layer formed so that the system could contain

more molecules than the nominal available slots. The results are shown in Figure 13. The second adsorbed layer is not formed until the chemical potential reaches -24.5. Lots of molecules have already been added to the system at a lower chemical potential, thus, the tight packing of molecules in the system reflects the adsorption compression phenomenon occurring. The adsorbate molecules repel each other as they are strongly attracted to the adsorbent surface while packed closely in the adsorbed layer. Figure 14 shows the relation between the number of molecules in the first layer versus the chemical potential at $\varepsilon_s/kT = -30$ and $\varepsilon/kT = -1.0$. At μ/kT -24.5 when the second adsorbed layer is formed, the number of adsorbed molecules has already increased to approximately the maximum number. Thus, not many molecules are added into the second adsorbed layer, but they are all adsorbed in the first layer, experiencing the adsorption compression phenomenon.

Figure 15 shows the average interaction energy between neighboring molecules in the first adsorbed layer as a function of chemical potential at $\varepsilon_s/kT = -30$ and $\varepsilon/kT = -1.0$. A positive value of the interaction energy indicates the repulsive interaction exists between the neighbors and a negative value of the interaction energy indicates the attractive interaction. The average interaction energy of the system turns to zero from negative value at $\mu/kT = -27$. As the chemical potential keeps increasing from $\mu/kT = -27$, the average interaction energy also increases. The slope of the curve represents the force between the neighboring molecules. The positive slope, indicating repulsive forces, occurs at $\mu/kT = -40$. Figure 15 provides another strong evidence of adsorption compression in adsorption system on a flat homogeneous surface.

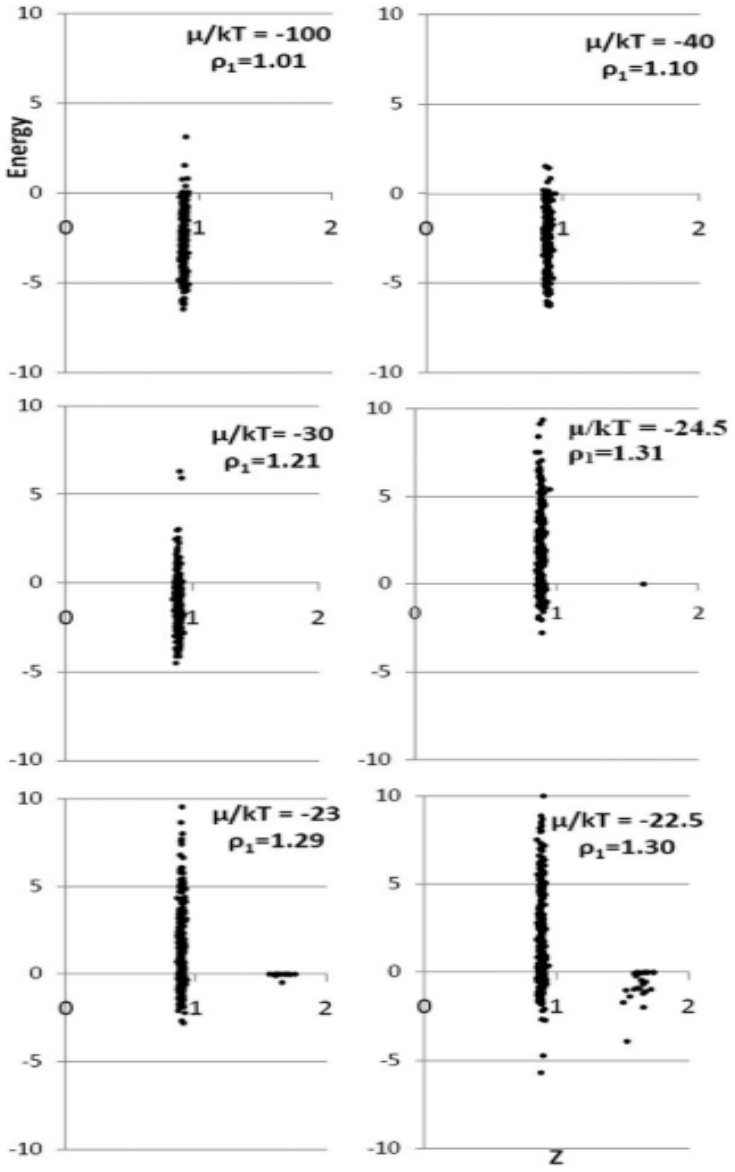

Figure 13: Energies of adsorbate–adsorbate interactions as a function of the distance, z, to the surface for different chemical potentials at ε/kT=-1.0 and ε_s/kT =-30. Values of ρ1 are normalized densities in the first layer.

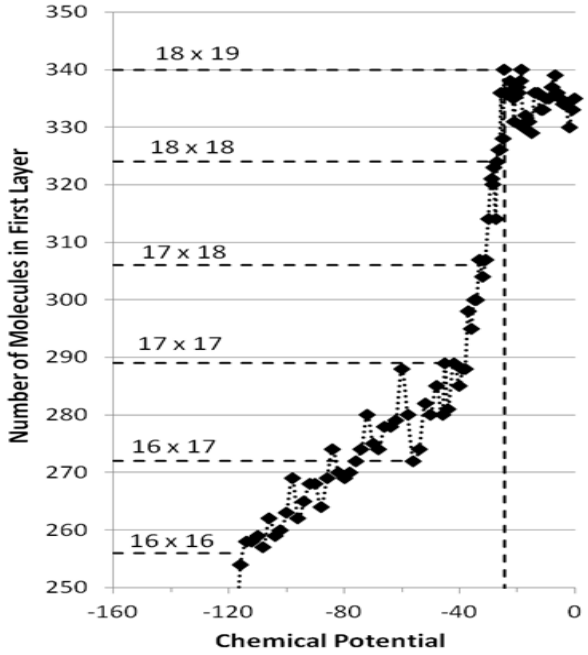

Figure 14: Number of the adsorbed molecules on the flat surface for ε/kT = -1.0, ε_s/kT = -30 and various μ/kT

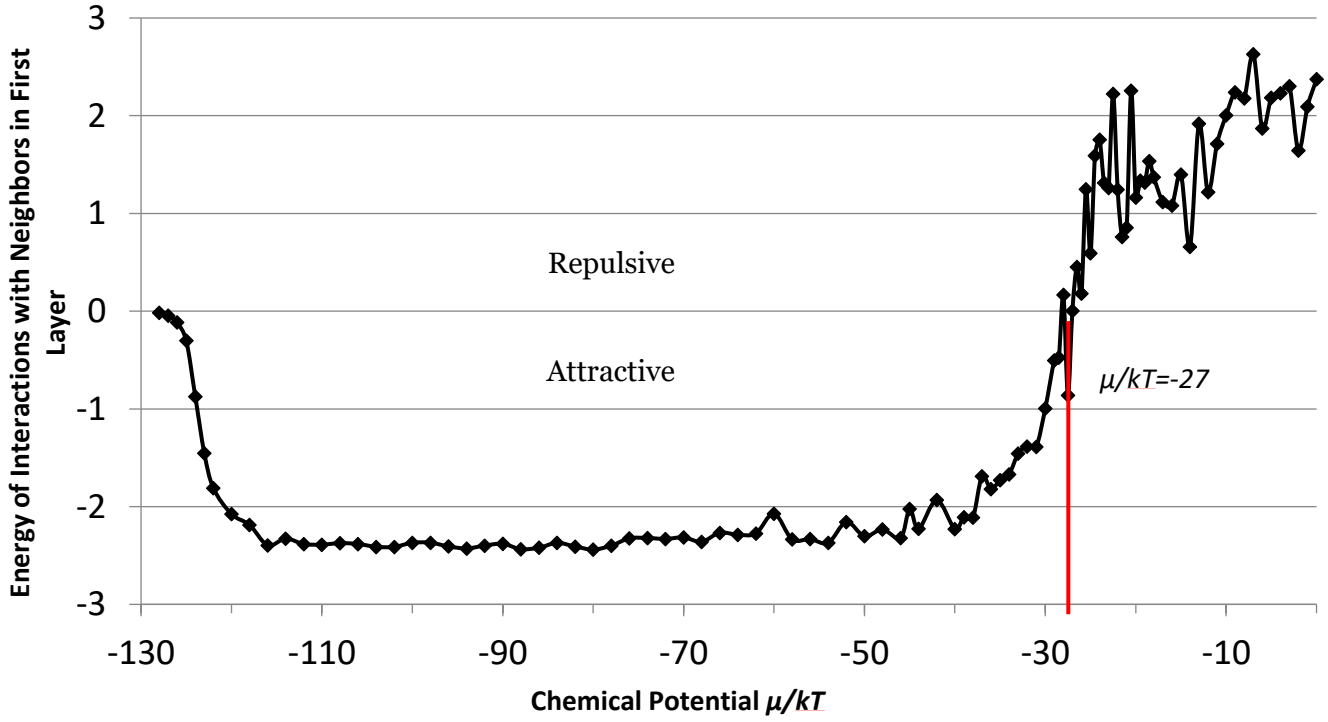

Figure 15: Average interaction energy between neighbors at various μ/kT

3. Experimental Study of Adsorption Compression with Temperature-Programmed Desorption (TPD) Experiment

This section will discuss the experimental methods used to obtain an adsorption isotherm of carbon monoxide (CO)- H-ZSM-5 adsorption system. AutoChem II 2920 Chemisoprtion Analyzer is equipped with Omnistar GSD 320 mass spectrometer (MS) to measure the signal of CO coming out from the sample tube into the thermal conductivity detector (TCD) and MS at a temperature of 35ºC. All data are collected with ASCII type file, and then later converted into Excel worksheet. Manual area integration of both chemisorption and physisorption peak under the MS curve is carried out in Excel to conduct a qualitative analysis of how much CO gas is adsorbed onto the H-ZSM-5 zeolites. The profile of the adsorption isotherm can be generated from the area data. The data is also plotted in the Ono-Kondo coordinates to determine whether adsorption compression exist in the CO/H-ZSM-5 system.

CO and Zeolite H-ZSM-5 System

Carbon monoxide (CO), accompanied with NO_x, is the main component found in the automobile emission and power plants. How to decompose the toxic NO_x and CO species out from the exhaust into less toxic and eco-friendly components has been studied recently. It is found that the metal-substituted zeolites might be potential catalysts that can be utilized in the decomposition catalytic reactions. Therefore, an adsorption experiment of CO or NO_x onto zeolites were conducted to check the performance of zeolites catalysts as well as to evaluate if there exists the adsorption compression phenomenon in the system. Since CO adsorption is used to be the probe of the cation loading in ion-exchange processes in zeolites[32] while nitrogen-containing gas species undergoes different types of reaction, such as NO disproportionation and $NO+O_2$ reaction, with the presence of zeolite[33], CO is selected as the adsorbate gas in these experiment to minimize the

potential side reactions that could influence the results. There are many different types of zeolites that could be selected as the adsorbent in the experiment. Zeolite H-ZSM-5 with a Si/Al ratio of 40 has been chosen to become the adsorbent. With literature support[34] and the potential applications consideration, CO and H-ZSM-5 adsorption system is used in the temperature-programmed desorption (TPD) experiment in order to measure the adsorption isotherm of CO on H-ZSM-5 at 35°C with different CO concentration, which simulates the automobile exhaust temperature to see how H-ZSM-5 will act as the adsorbent along with CO adsorbate.

Experimental Design and Method

Temperature-programmed desorption (TPD) experiments are conducted using CO as the adsorbate and H-ZSM-5 as the adsorbent to measure the adsorption isotherm. The TPD experiments is conducted using AutoChem II 2920 Chemisorption Analyzer (AutoChem). The equipment allows various types of temperature-programmed experiments, BET surface area analysis along with pulse chemisorption experiments. Thermal conductivity detector is used to detect the difference in gas component between the Reference stream and Carrier stream. By converting thermal conductivity difference into signal, the paired computer software MicroActive could display the results and recorded the data. Experimental procedure setup, analysis of the experiment, experiment parameter settings, and monitoring experiment process are all done with the MicroActive software. Figure 16 shows the schematic of the MicroActive software user interface and the structure inside of the equipment. The green line represents the Preparation gas stream where the preparation gas flow into the sample tube and leave the equipment directly through the exhaust streamline without getting into the TCD detector. This design is used to prevent any potential damage to the TCD filament as some pretreatment gases may oxidize the filament. The blue line represents the Reference and Carrier gas stream. Both of these two streams

go through the TCD, and the TCD signal is measured depending on the difference in thermal conductivity between the Reference and Carrier. Usually the inert noble gas, such as Helium and Argon, are used in Reference and Carrier stream line for consistent signal processing. The red line represents the Loop gas stream where target adsorbate gas can mix with the Carrier gas to adjust to different adsorbate concentrations.

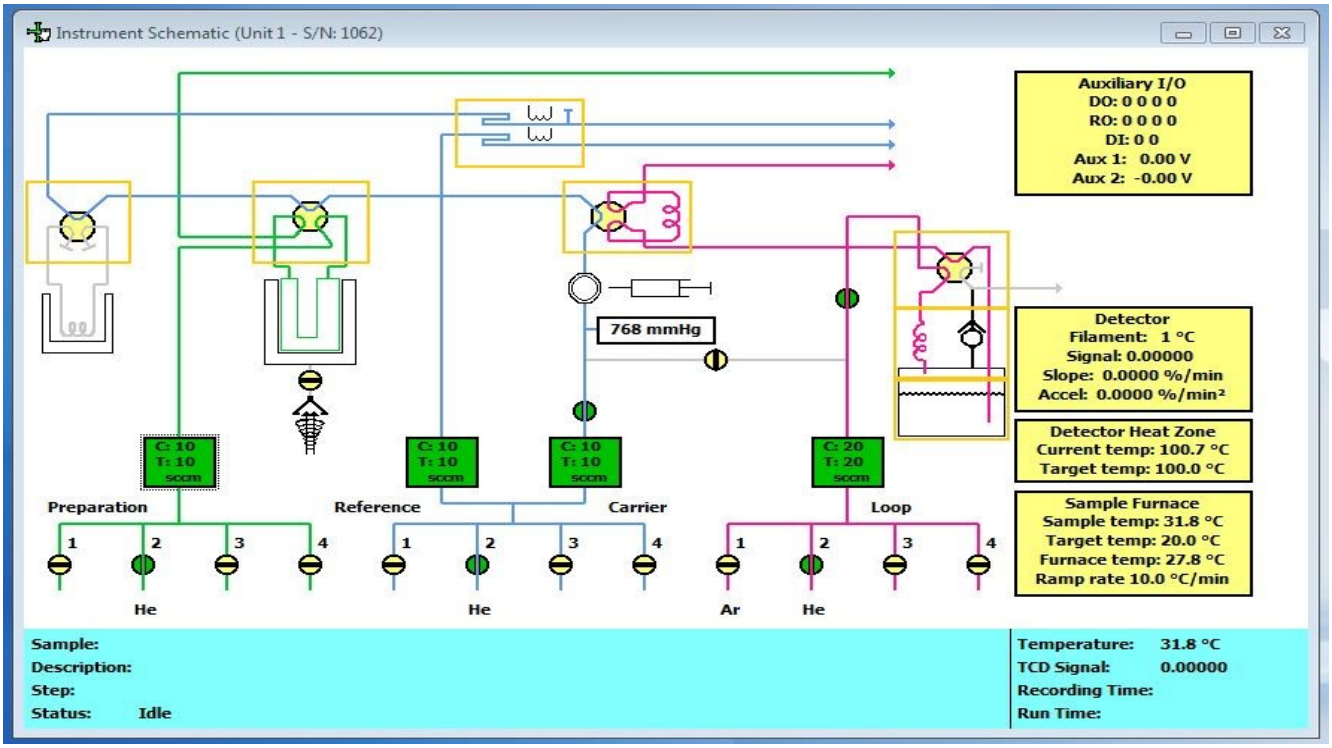

Figure 16: Schematic of MicroActive user interface

Besides the gas streams, there are many other elements that have different functions in the equipment. The circle with a straight line lying in the middle represents the controllable valve enabling operators to change the gas stream flow status under the manual control mode. The yellow box with a six-way valve inside represents the cold trap valve, analysis valve, loop valve, and vapor valve from left to right respectively. The cold trap valve controls the Carrier gas flow either enter the cold trap (grey spiral line) cooled with liquid nitrogen and iso-propanol mixture or bypass it. It is not used in TPD experiments. The analysis valve controls the carrier gas to flow through

the sample tube, which is the U-shape device beneath the yellow valve region or bypass it. A KwikCool cooling system is attached to the sample chamber. The KwikCool blows in air cooled with ice-water mixture to achieve the goal of cooling. When the Carrier gas is not supposed to enter the sample tube, analysis valve can be used to ensure the gas stream bypasses the sample. The Loop valve is mostly used in pulse chemisorption, it controls the injection of Loop gas into the Carrier stream line in the manner of pulse. Vapor valve is rarely used as experiment that requires the vapor generator is not common. The TCD detector is shown in the top middle yellow box with two filaments. Each yellow box is a heat zone where the temperature can be controlled either manually or via a preset program to achieve the experimental condition. The rectangular boxes with numbers in it are mass flow controllers (MFCs), alphabet C in the box shows the current flow reading while alphabet T in the box shows the target flow rate. Both readings are in the units of standard cubic centimeter per minute (sccm). MFCs need to specify the flowing gas species to record an accurate reading value. This could be achievement using MicroActive software.

An OmniStar GSD 320 mass spectrometer (MS) is connected to the AutoChem to track the gas component coming out of the sample tube. The MS is very sensitive to the surrounding environment and it can detect trace amount of specified gas species. The MS draws one standard cubic centimeter per minute (sccm) gas sample from the AutoChem into the capillary tube. Then the gas will be pumped down to high vacuum after entering the inlet valve and to an even lower pressure in the filament chamber to get ionized. This enables the ions to travel further in the vacuum by reducing the possibility of collision. After ionization, the gas sample will go through a quadruple mass filter and the ions with the selected mass to charge ratio will be detected. Only the ions with the selected mass to charge (m/e) ratio will get detected, other ions will deflect into other directions away from the detector. Figure 17 and 18 shows the schematic of MS and the working

mechanism of quadruple mass filter. The lab view of the whole set of equipment is show in in Figure 19. A water trap is used to remove residue water content connected to Loop gas cylinder in the back.

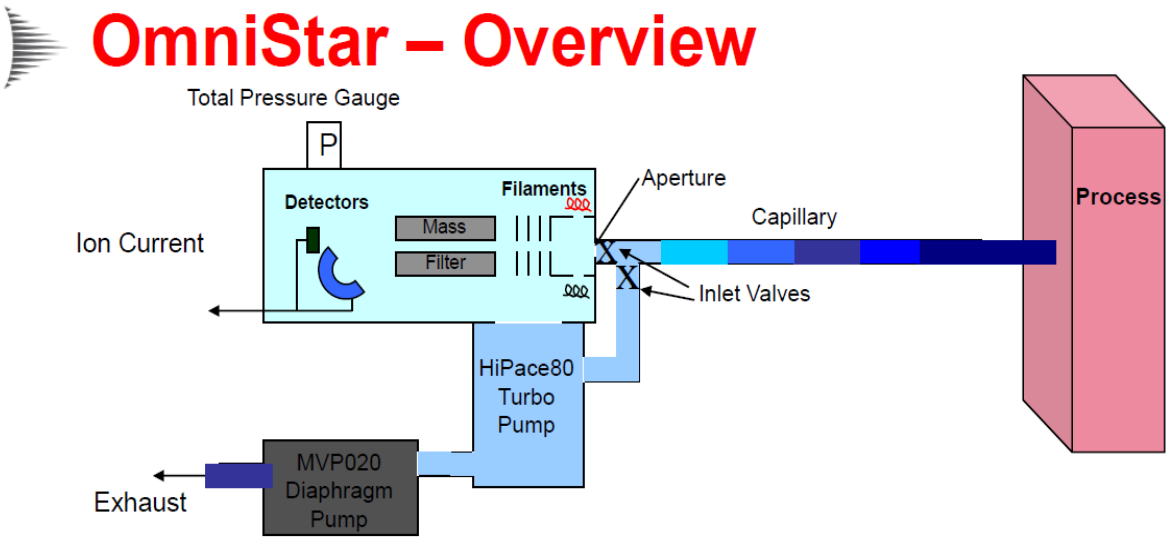

Figure 17: Schematic of Omnistar GSD 320 Mass Spectrometer

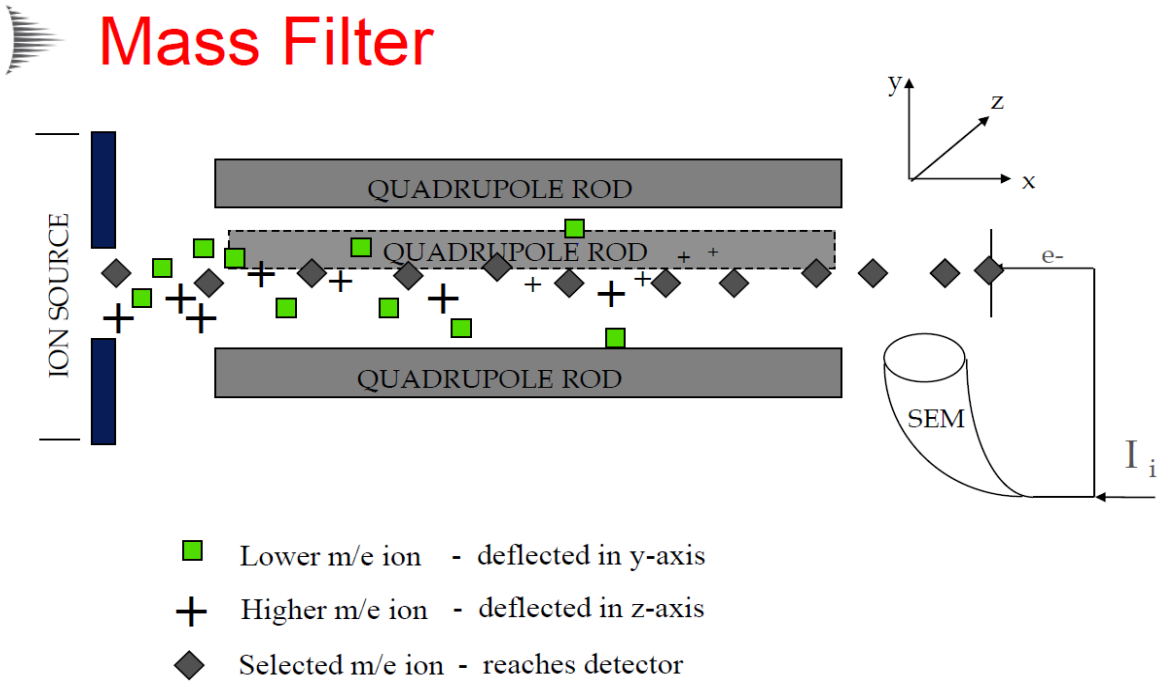

Figure 18: Working Mechanism of Mass Filter in MS

Figure 19: Lab view of AutoChem and MS

The TPD experimental procedure consists of 4 main parts: pretreatment of the sample H-ZSM-5, adsorption of CO-He gas mixture at different concentrations, sample flush with He to remove physisorbed CO species, and sample temperature ramp to measure chemisorbed CO species. The H-ZSM-5 sample with a Si/Al ratio of 40 is supplied by Dr. Pengfei Xie from Dr. Chao Wang's group. It is white granular powder with different sizes. In literature, H-ZSM-5 zeolites are prepared by ion-exchange of Na-ZSM-5 for 24 hours with 2M of NH_4NO_3 solution with a zeolite to solution ratio of 1 g zeolite/10 cm^3 solution at 353K to get NH_4^+-ZSM-5. After ion exchange, the NH_4^+-ZSM-5 was filtered, washed with de-ionized water, and calcined at 823K for 3 hours under airflow to decompose the ammonium ions to produce hydrogen form[35]. All gases used in the experiments were from Airgas company.

Before loading the H-ZSM-5 sample into the U-shape sample tube, quartz wool is placed in the bottom of the large diameter side to prevent particles movements into the small diameter side and clog the equipment. Around 0.1000g ($\pm 0.0005g$) sample is loaded into the sample tube

using the electronic balance. The same sample is used repetitively for all concentration profiles to ensure the consistency in zeolite structure and properties as well as the accuracy of the data. After installing the sample tube into AutoChem equipment, TPD analysis is started with the set program. The first part, the pretreatment of the sample, is required only when new H-ZSM-5 sample is loaded. Otherwise, the pretreatment of sample is skipped during multiple repetitions. During the pretreatment, the sample is constantly under Helium gas flow. It is first heated up to 800ºC at 10ºC/min and hold for 8 hours to remove the remaining water content. After the sample temperature returns to 70ºC with KwikCool cooling system, a second calcination to 1000ºC at 10ºC/min and hold for 30 minutes is conducted to further remove the water content. Afterwards, the sample is returned to 35ºC and is ready for CO adsorption. Figure 20 shows the MS graph during the pretreatment of H-ZSM-5 sample in He gas flows under log scale. The black curve represents the water signal of mass 18. During the first calcination, there are two water peaks appearing. The first one (a) occurs at 100ºC as the boiling point of molecular water, the second peak (b) occurs at around 625ºC, which might be the structural -OH group in H-ZSM-5. The water

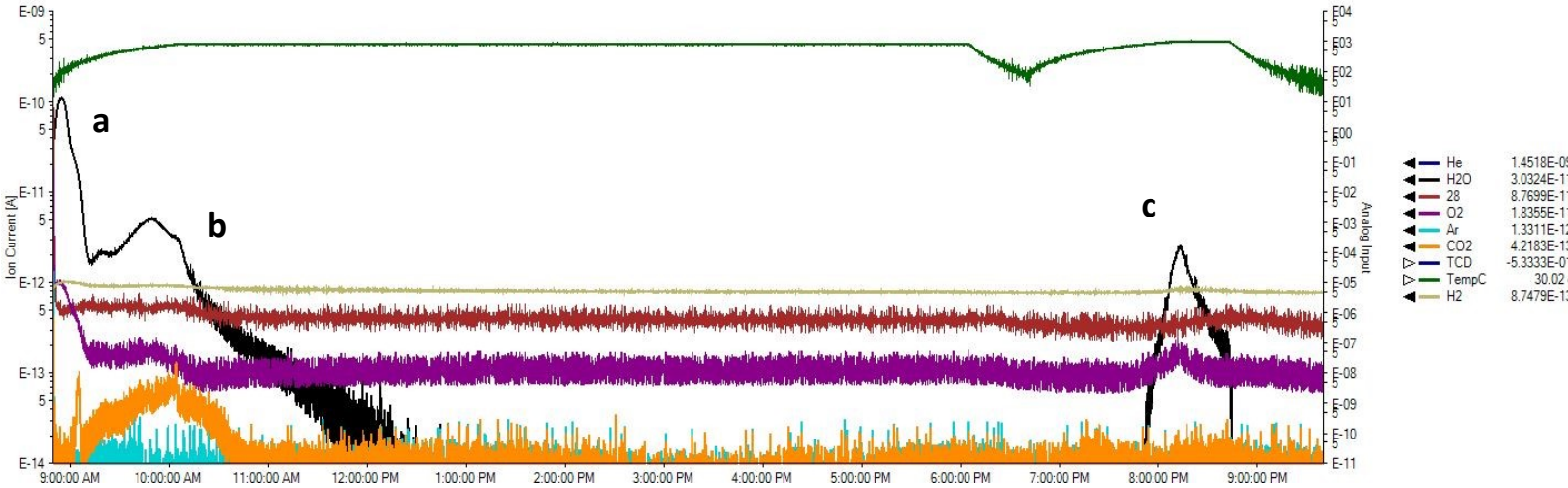

Figure 20: MS graph of pretreatment of the sample by heating up 800ºC for 8 hours with second calcination at 1000ºC for 30 minutes in logarithm scale.
9.981% CO-He, 01-12-2019

After pretreatment, the sample is then fed with CO-He mixture gas for adsorption at 35 ºC. For low concentration of CO starting from 500 ppm and below, in order to reach a stable flat curve in MS, a waiting time for 3 hours is employed. For higher concentration above 500 ppm, a 3-hour waiting time is used to reach an ad/desorption equilibrium in the sample tube. The CO-He gas mixture is blended using the Loop CO gas balanced with He and Carrier He gas to adjust to different concentrations interested in the experiment. The mixing ratio is calculated manually and then input into the MicroActive software so that the MFCs can control the mass flow rate with accuracy. There are 4 different CO gas cylinders used in the experiment. 50 ppm, 500 ppm, 5000 ppm, and 10% CO-He balanced gas cylinder are used to carry out the experiment to measure the adsorption isotherm starting from 3.5 ppm to 10%. For each gas cylinder, 8 concentration profiles, starting from high to low, with 100%, 80%, 60%, 40%, 20%,15%,10%, and 7% of the marked concentration are tested as one experiment series. In one experiment series with one CO-He balanced gas cylinder, the procedure starts from high concentration to low concentration, i.e., for 10% CO-He gas cylinder, the experiment will conduct 10% Co-He TPD experiment first, followed by 8%, 6%,4%,2%,1.5%, 1% and 0.7% CO-He TPD experiments. The TPD experiments for the first concentration profile is repeated six times when new H-ZSM-5 sample is loaded to obtain consistent results in chemisorption area calculations.

Next, pure He gas from Carrier gas stream will be used to flush the sample for two hours at the same temperature as the CO adsorption stage. This is to ensure that all weakly physisorbed CO species will be removed from the H-ZSM-5 so that the physisorbed species will not be counted as chemisorbed species. The removed physisorbed CO species will later get detected in MS to calculate the physisorbed CO peak area.

After flushing, a temperature ramp of the sample is conducted at 10°C per minute until the sample reaches 500°C, and the temperature will hold for an hour before returning to 35°C and repeat the procedure for different concentrations. Figure 21 shows the MS graph of two full cycles of a TPD experiment without pretreatment. The brown curve is the CO signal of mass unit 28. The CO curve goes up as the CO-He mixture is fed into the sample. The adsorption stage (a) lasts for 3 hours so that the CO curve can reach a constant level. After that, pure He gas is flushing through the sample tube as the CO curve on MS graph returns to the baseline. This is the point where physisorption data is obtained. The flushing stage (b) lasts 2 hours following the temperature ramp (c) to remove the chemisorbed CO species. The green curve on top of the curve represents the temperature in the sample tube. At the beginning of the temperature ramp stage (c), the CO curve displays a peak, highlighted in red circle. These peaks are regarded as the desorption of chemisorbed CO species. The temperature ramp stage will hold at 500°C for an hour, and the same procedure will be repeated with a different CO adsorption concentration.

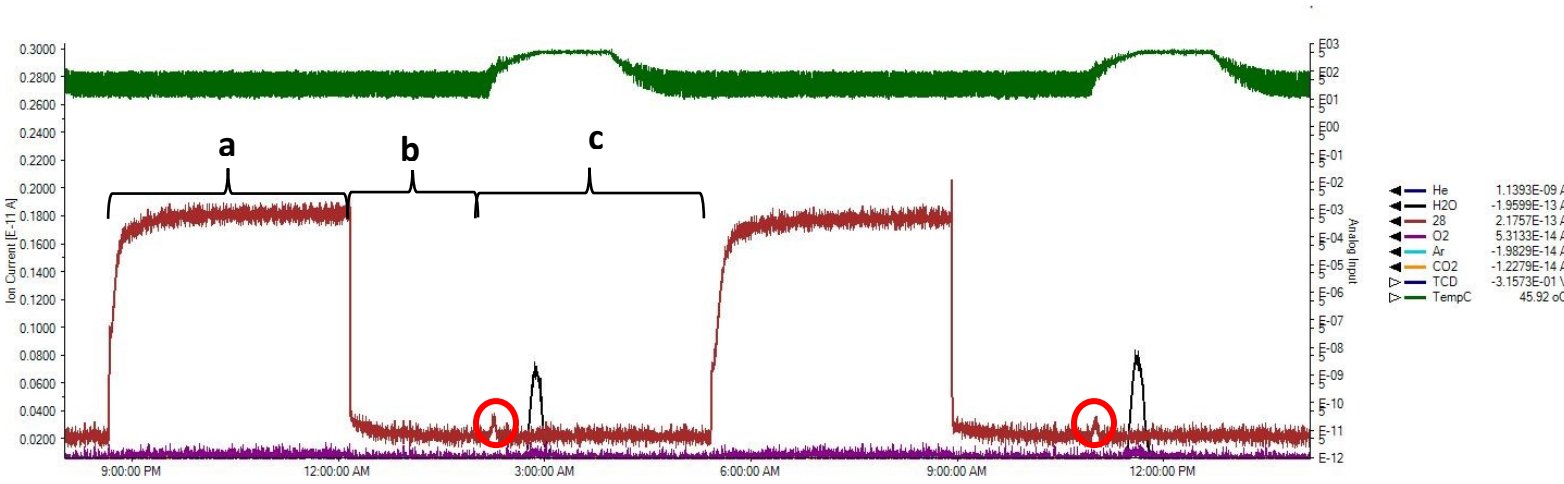

Figure 21: MS graph of CO adsorption stage (a), He flush stage (b), and temperature ramp stage (c) for two cycles in linear scale.
50 ppm CO-He, 03-04-2019

MS Data Analysis

The data obtained using MS can be retrieved first in ASCII file. The file later can be converted into Microsoft Excel spreadsheet to manually integrate the area corresponding to the physisorption and chemisorption CO species. An adsorption isotherm can be generated using the area data, and by plotting the isotherm into the Ono-Kondo coordinates, the characteristic of the adsorbate-adsorbate interaction can be summarized with the slope of the curve. Figure 22 shows how physisorption area is obtained using Microsoft Excel. After converting data in an Excel spreadsheet, the physisorbed CO isotherm can be constructed by plotting the signal in mbar versus the time in second. To simplify the calculation, the time axis has been set such that the beginning time of He flush stage, which is also the time when CO curve starts dropping, is 500 to make sure the CO MS curve for different concentrations can be plotted and compared in the same plot. The MicroActive software has the experiment log that records the beginning time of each stage when He is used to flush out the weakly physisorbed CO species for physisorption calculation. This time can be mapped onto the Excel spreadsheet. The data are collected starting from 500 seconds prior to the time so that one can make sure whether the adsorption system has reached equilibrium. The total time period of the data collection lasts 3000 seconds, which is 50 minutes, to ensure that a stabilized CO baseline is obtained at the end of the curve. A vertical line is drawn at the time when He gas starts flowing and a horizontal line is extended to the left from the CO baseline at the end of the curve. These two lines intersect and form a closed area below the CO curve. The area under the curve is interpreted as the physisorption area. Manually integrate this area using trapezoid law provides a numerical value of how much physisorbed CO species has come out from the sample and get detected in MS.

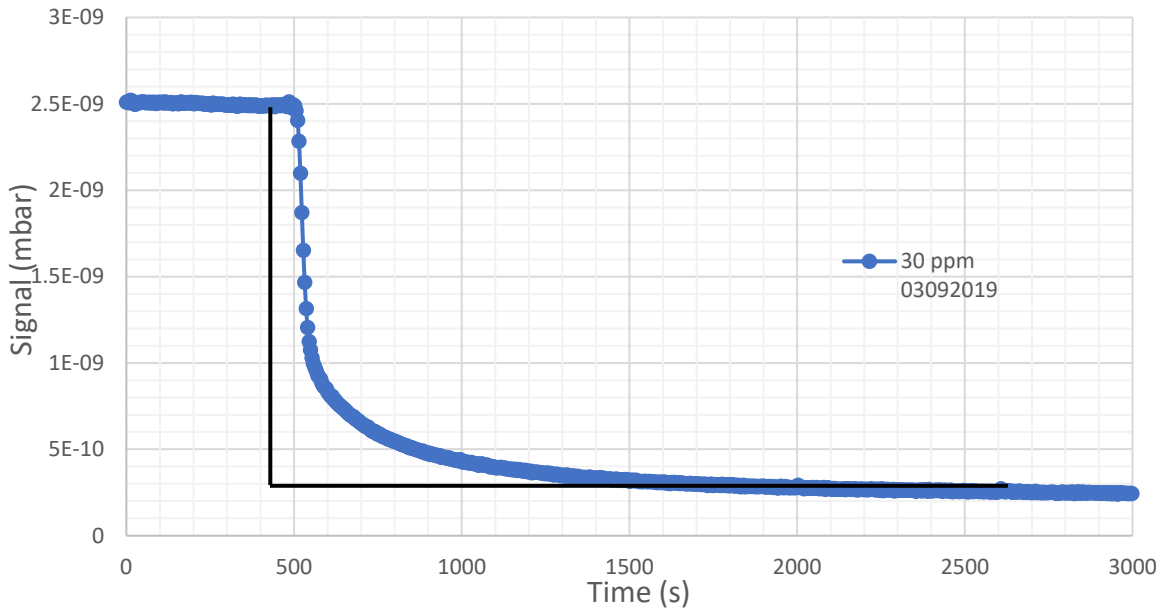

Figure 22: Determination of physisorbed CO area in Excel.
30 ppm CO-He, 03-09-2019

Similarly, using the same technique, the area of the chemisorbed CO peak can be retrieved in Excel by constructing a baseline between the beginning of CO desorption point and the end of the peak. The peak area then can be calculated. Figure 23 shows the process of the calculation.

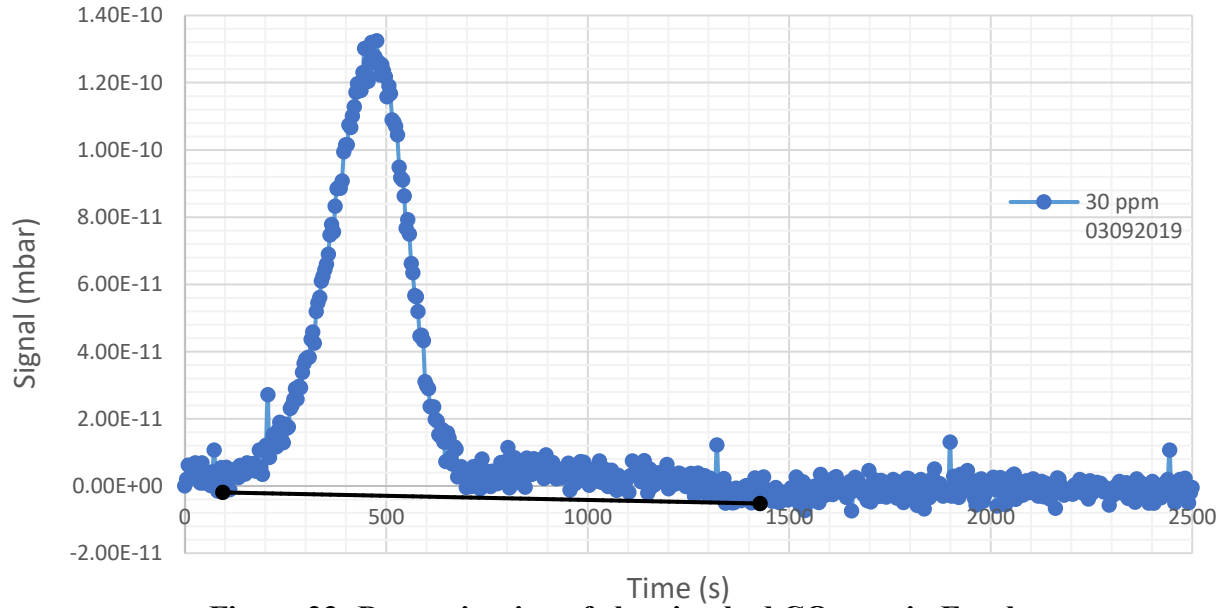

Figure 23: Determination of chemisorbed CO area in Excel.
30 ppm CO-He, 03-09-2019

The calculated area data then can be plotted together to construct the adsorption isotherm for further study. Figure 24 shows the curve of physisorption area with respect to CO concentration in linear scale. From 3 .5 ppm to 10% CO gas concentration, a total of 27 data points has been collected to construct the physisorption isotherm of CO at 35ºC. The red data points represent the concentration profile gathered in 10% CO-He experiments while the brown, green, and blue data points represent CO concentration of 5000 ppm, 500 ppm, and 50 ppm experiments respectively. In all collected data, data points for 35, 75, and 100 ppm are a bit off from the general trend due to the experiment error. At low concentration range below 100 ppm, the physisorption peak area rises quite rapidly. When CO concentration increases to 350 ppm, the curve rises slowly until 5000 ppm compared to the trend in low concentration range. Starting from 0.7% CO concentration, the curve resumes to rise at a steep slope. Since not all concentration during the interval from 3.5 ppm to 10% have been tested, there could be different behavior of the physisorption area curve if putting these untested concentrations into consideration. Nonetheless, Figure 24 provides useful information about physisorption peak area which can be later plotted into the Ono-Kondo coordinates. Figure 25 shows the same data as in Figure 24 with x-axis plotted in logarithm scale. Table 2 lists the physisorption peak value calculated with the corresponding CO concentration.

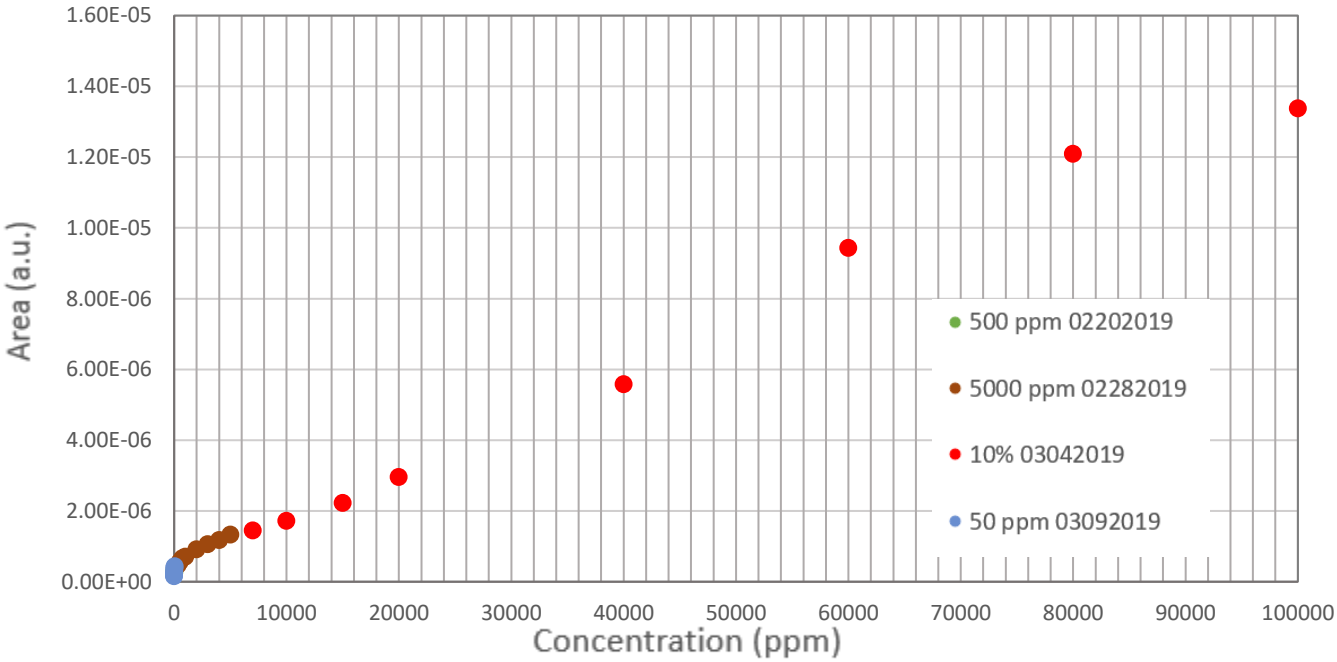

Figure 24: Physisorption peak area of CO on H-ZSM-5 with concentration from 3.5 ppm to 10% in linear scale

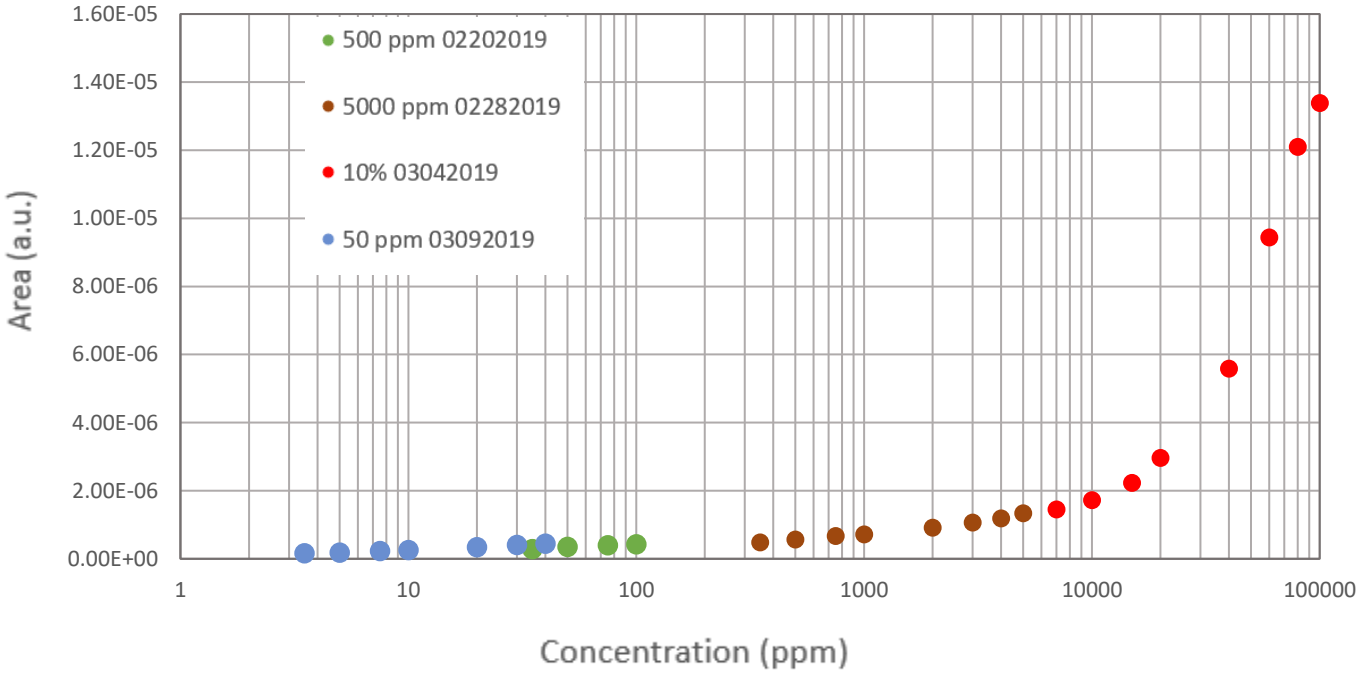

Figure 25: Physisorption peak area of CO on H-ZSM-5 with concentration from 3.5 ppm to 10% in logarithm scale

Table 2: Physisorption peak area of CO with corresponding CO concentrations

Concentration (ppm)	Area (a.u.)
100000	1.338E-05
80000	1.209E-05
60000	9.437E-06
40000	5.583E-06
20000	2.956E-06
15000	2.222E-06
10000	1.718E-06
7000	1.447E-06
5000	1.334E-06
4000	1.180E-06
3000	1.059E-06
2000	9.137E-07
1000	7.077E-07
750	6.615E-07
500	5.581E-07
350	4.732E-07
100	4.157E-07
75	3.898E-07
50	3.465E-07
40	4.373E-07
35	2.748E-07
30	3.995E-07
20	3.396E-07
10	2.552E-07
7.5	2.265E-07

5	1.804E-07
3.5	1.531E-07

Figure 26 shows the chemisorption peak area of different CO concentrations. The data points on the graph is hard to see at low concentration in linear scale, so the same graph is plotted with x-axis in logarithm scale and is shown in Figure 27. Identical to the legends in physisorption area figure, the red, brown, green, and blue data points correspond to 10%, 5000 ppm, 500 ppm and 50 ppm CO TPD experiments respectively.

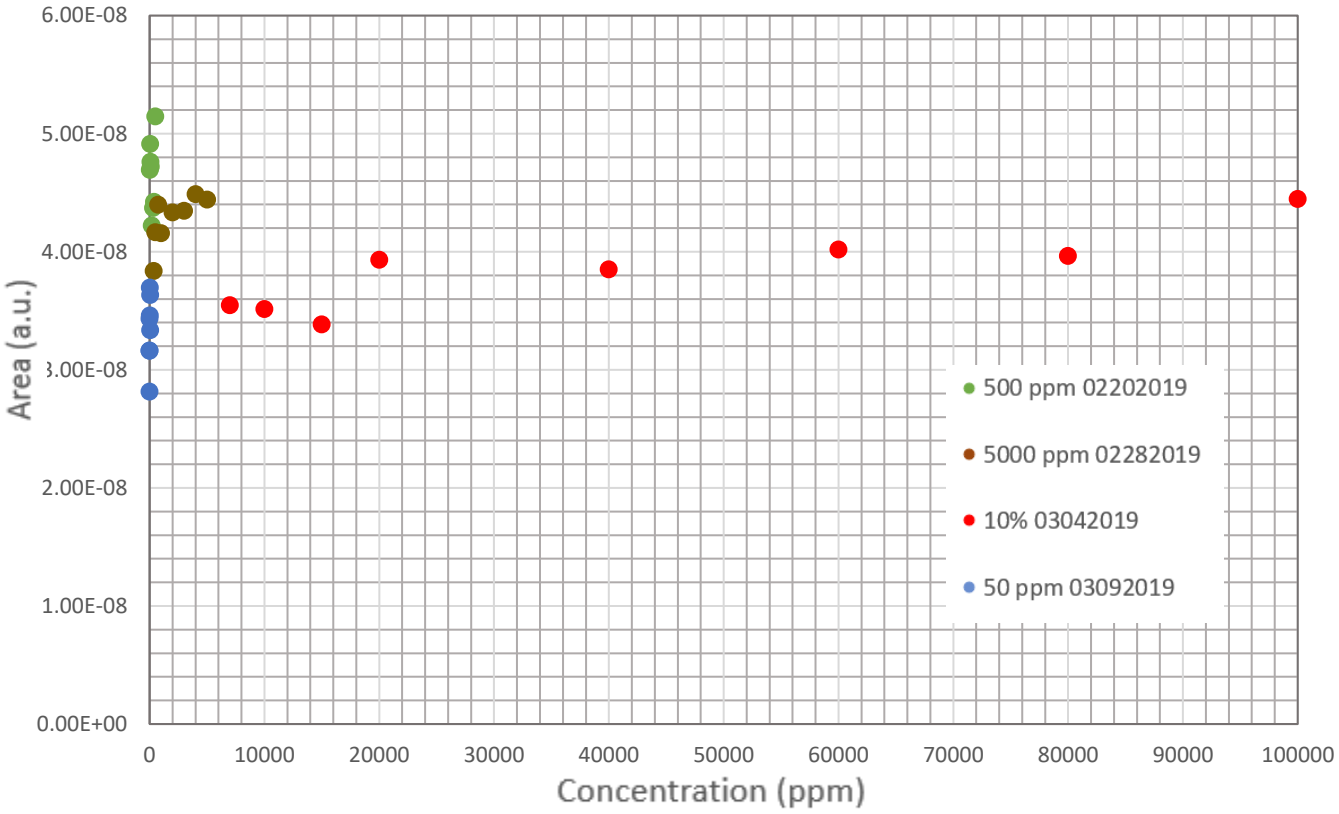

Figure 26: Chemisorption peak area of CO on H-ZSM-5 with concentration from 3.5 ppm to 10% in linear scale

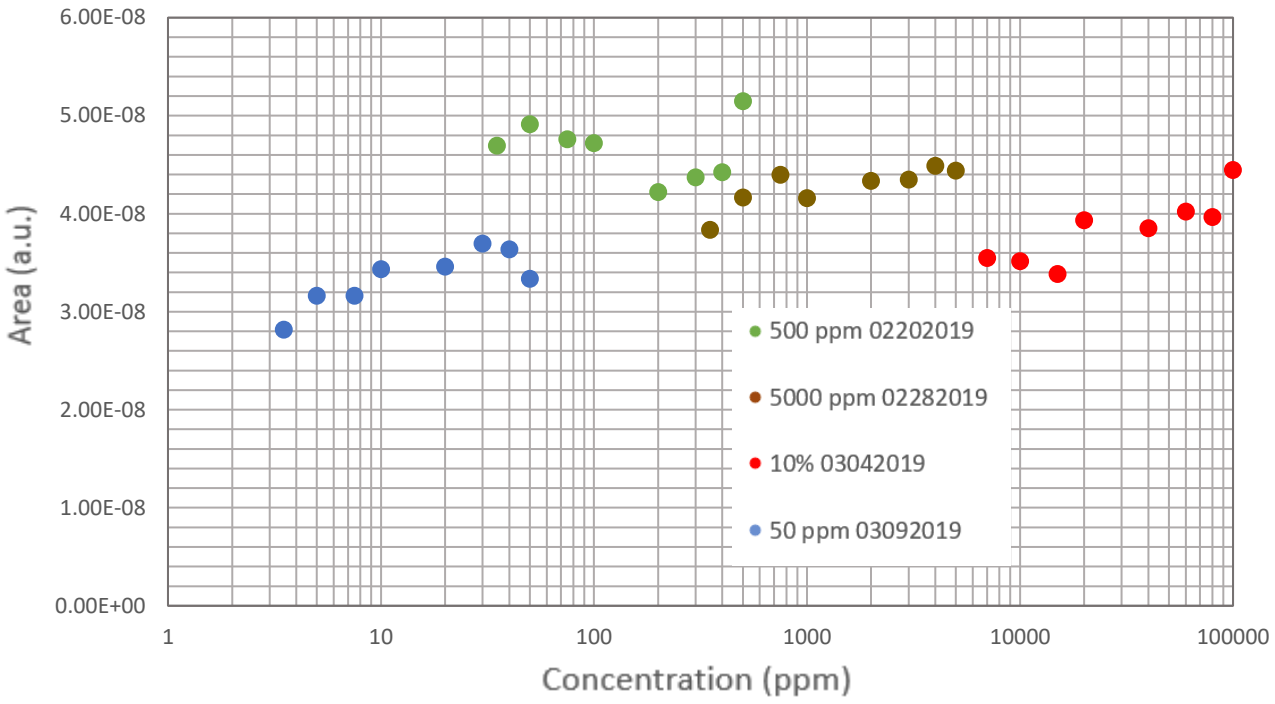

Figure 27: Chemisorption peak area of CO on H-ZSM-5 with concentration from 3.5 ppm to 10% in logarithm scale

The chemisorption peak areas, unlike physisorption case where there is a clear trend of increasing peak area along with the CO concentrations, maintain at a constant value in the range of $3\sim5\times10^{-8}$. As the same H-ZSM-5 sample has been used consecutively for several experiments with different CO concentrations, the chemisorption peak area gradually decreases according to the time order of the experiments. This may indicate the aging or defects of H-ZSM-5 active site for CO chemisorption after multiple usages and repetitive heating procedures. There are 30 entries of chemisorption peak area data and they are listed in Table 3 with the corresponding CO concentration.

Table 3: Chemisorption peak area of CO with corresponding CO concentrations

Concentration (ppm)	Area (a.u.)
100000	4.447E-08
80000	3.965E-08
60000	4.020E-08
40000	3.850E-08
20000	3.933E-08
15000	3.384E-08
10000	3.516E-08
7000	3.547E-08
5000	4.441E-08
4000	4.487E-08
3000	4.346E-08
2000	4.334E-08
1000	4.157E-08
750	4.398E-08
500	4.165E-08
400	4.422E-08
350	3.836E-08
300	4.371E-08
200	4.222E-08
100	4.720E-08
75	4.760E-08
50	4.914E-08
40	3.635E-08
35	4.693E-08
30	3.696E-08
20	3.459E-08

10	**3.434E-08**
7.5	**3.163E-08**
5	**3.162E-08**
3.5	**2.816E-08**

After constructing both physisorption isotherm and chemisorption isotherm, the isotherm data can be plotted into Ono-Kondo equation (Eqn.[11]) to check the characteristic of the interaction energy between the adsorbate molecules in the adsorbed layer. Figure 28 shows the physisorption isotherm of different sets of concentration plotted in Ono-Kondo coordinates. The curve in Ono-Kondo coordinates displays a steep negative slope for 3.5-50 ppm and 350-5000 ppm CO experiments, the slope of the curve slowly approaches to zero for 0.7% to 10% CO experiments. A negative slope in Ono-Kondo coordinates indicates a repulsive energy experiencing by the adsorbate molecules in the adsorbed layer. One reason why the slope closes to zero as CO adsorbate concentration in bulk increases is that such a high concentration profile leads to larger repulsive energy and the adsorbate-adsorbent attractive interaction cannot compensate this repulsive energy, so CO molecules cannot be adsorbed onto the surface as adsorption compression phenomenon disappears. Figure 29 shows the chemisorption isotherm in Ono-Kondo coordinate, the scattering data points in Ono-Kondo coordinate cannot tell much information, but for each set of concentration profiles, the curve still shows negative slope, indicating repulsive interaction in the adsorbed layer and the existence of adsorption compression phenomenon.

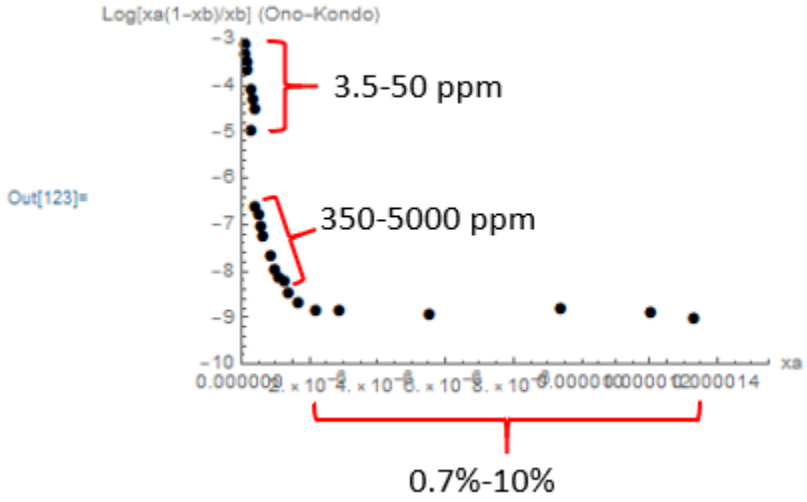

Figure 28: CO physisorption isotherm in Ono-Kondo coordinate for concentration from 3.5 ppm to 10%

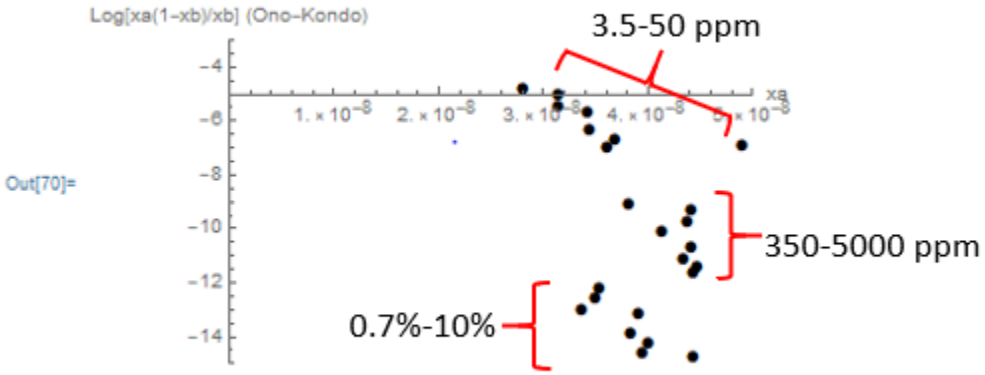

Figure 29: CO chemisorption isotherm in Ono-Kondo coordinate for concentration from 3.5 ppm to 10%

4. Conclusion

Adsorption compression is observed in GCMC simulation of molecules adsorbing on a flat surface when $\varepsilon_s/kT = -30$ and $\varepsilon/kT = -1$. The number of molecules adsorbed in the adsorbed layer has exceeded the arrangement limits, however, no second adsorption layer has been observed based on simulation data. This result indicates the adsorption compression phenomenon occurs in the first adsorbed layer so that the adsorbed molecules can pack closer to each other and let more adsorbate molecules adhere to the surface. Energy of interaction data between neighboring molecules also supports that the adsorption compression occurs when the interacting forces between neighboring molecules is repulsive starting from $\mu/kT = -40$.

Adsorption isotherm data of CO-H-ZSM-5 adsorption system at 35ºC is collected using AutoChem II 2920 Chemisorption Analyzer paired with Omnistar GSD 320 mass spectrometer. By plotting the adsorption isotherm data into Ono-Kondo coordinates, the negative slope in low concentration range between 3.5 to 5000 ppm of the curve represents a repulsive interaction existed between the adsorbate molecules. The results show that the adsorption compression also occurs in CO-H-ZSM-5 system at concentration between 3.5 ppm to 5000 ppm at 35ºC.

Appendix

Mathematica code for 2-D Canonical Ensemble simulation

```
(*Generate a random configuration of n pts in a m by m coordinates*)
(*For simplification,pick n=200,m=100*)
(*Try to get rid of repeated {x,y} combinations*)


m = 100;(*Size of the matrix*)
n = 500;(*Number of points*)
Itr = 5000;(*Number of iterations*)


PTS = Table[RandomInteger[m, {2}], n];(*Generate a table with 100 randomized {x,y} pairs*)

For[q = 1, q ≤ 2, q++
   (*Check if there are any repeating pts*)
   Do[
    If[DuplicateFreeQ[PTS[[All, 1]] && PTS[[All, 2]]] == True, Dup = 0, Dup = 1];
    (*Need check if the criteria would always hold true*)
    (*Check any duplicates pairs of {x,y}*)
    If[Dup == 0, PTS = PTS, PTS = Table[RandomInteger[m, {2}], n]];(*Change to a new config*)
    , {i, 1, 5}]; (*Iterate five times if the generated pts have identical values*)

PTS1 = PTS; (*Store the alternated config*)

(*L-J potential parameters*)(*Assume parameter's values, change later as needed*)
epsilon = 1.0;
sigma = 1.0;
ener1 = 0; (*Initial/Proposed step energy counter*)
ener2 = 0;
num11 = 0; (*Number counters for the nearest neighbours*)
num21 = 0;
num12 = 0;
num22 = 0;
c = 1; (*Counters of pts*)
d = 1;


(*Assume the lattice and a distance of 1 between two junction*)
RR1 = 1; (*Distance of closest 4 neightbours*)
RR2 = Sqrt[2]; (*Distance of 4 second closest neighbours*)
```

```
(*Assume the lattice and a distance of 1 between two junction*)
RR1 = 1; (*Distance of closest 4 neightbours*)
RR2 = Sqrt[2]; (*Distance of 4 second closest neighbours*)

(*Calculate the number of 8 nearest neighbors for the whole config*)
Do[
 Do[
   If[Norm[PTS[[i, 1]]] - Norm[PTS[[c, 1]]] == 0 && Abs[Norm[PTS[[i, 2]]] - Norm[PTS[[c, 2]]]] == 1, num11 = num11 + 1];
   (*Closest 4 pts: Case 1: Same x, different y*)
   If[Norm[PTS[[i, 2]]] - Norm[PTS[[c, 2]]] == 0 && Abs[Norm[PTS[[i, 1]]] - Norm[PTS[[c, 1]]]] == 1, num11 = num11 + 1];
   (*Closest 4 pts: Case 2: Same y, different x*)
   If[Abs[Norm[PTS[[i, 1]]] - Norm[PTS[[c, 1]]]] == 1 && Abs[Norm[PTS[[i, 2]]] - Norm[PTS[[c, 2]]]] == 1, num21 = num21 + 1]
   (*Second closest 4 pts*)
   , {i, 1, n}];
 , {c, 1, n}];
ener1 = ener1 + 4 * epsilon * (num1 * ((sigma / RR1) ^12 - (sigma / RR1) ^6) + num2 * ((sigma / RR2) ^12 - (sigma / RR2) ^6));
(*Calculate potential of j for the original config*)


j = RandomInteger[n]; (*Pick a random pt*)
(*Move the randomed picked pt to a random position*)
PTS1[[j, 1]] = RandomInteger[{0, 100}];
PTS1[[j, 2]] = RandomInteger[{0, 100}];
(*Check if the new site is preoccupied*)
If[DuplicateFreeQ[PTS1[[All, 1]] && PTS1[[All, 2]]] == True, Dup = 0, Dup = 1];
(*Need check if the criteria would always hold true*)
(*Check any duplicates pairs of {x,y}*)
If[Dup == 0, PTS1 = PTS1, Goto[point2]]; (*Iteration number +1 if the site is occupied*)

(*Calculate the new potential*)
Do[
 Do[
   If[Norm[PTS1[[i, 1]]] - Norm[PTS1[[d, 1]]] == 0 && Abs[Norm[PTS1[[i, 2]]] - Norm[PTS1[[d, 2]]]] == 1, num12 = num12 + 1];
   (*Closest 4 pts: Case 1: Same x, different y*)
   If[Norm[PTS1[[i, 2]]] - Norm[PTS1[[d, 2]]] == 0 && Abs[Norm[PTS1[[i, 1]]] - Norm[PTS1[[d, 1]]]] == 1, num12 = num12 + 1];
   (*Closest 4 pts: Case 2: Same y, different x*)
   If[Abs[Norm[PTS1[[i, 1]]] - Norm[PTS1[[d, 1]]]] == 1 && Abs[Norm[PTS1[[i, 2]]] - Norm[PTS1[[d, 2]]]] == 1, num22 = num22 + 1]
   (*Second closest 4 pts*)
   , {i, 1, n}];
 , {d, 1, n}];
ener2 = ener2 + 4 * epsilon * (num1 * ((sigma / RR1) ^12 - (sigma / RR1) ^6) + num2 * ((sigma / RR2) ^12 - (sigma / RR2) ^6));
(*Calculate potential of j for the original config*)
```

```
 R = ener2 / ener1; (*Potential ratio of the proposed new cofig over original cofig*)
 If[R >= 1, PTS = PTS, (*If the new config has a higher potential, keep the original config*)
  If[R < RandomReal[], PTS = PTS1] (*Otherwise, compare the ratio of potential to a randomed value between 0 and 1.
    If the ratio R is smaller, switch to the new config*)
 ];
];
```

```
ListPlot[PTS, PlotStyle → PointSize[Medium], PlotLabel → 2 D MC, GridLines → Automatic, Frame → True, GridLinesStyle → Directive[Dashed]]
Timing[ListPlot[PTS]]
```

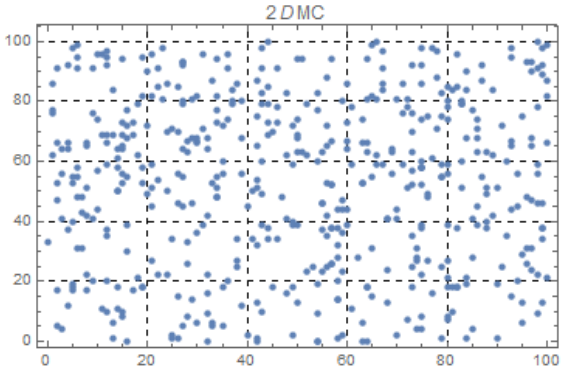

Adsorption isotherm in Ono-Kondo coordinate

```
q1 = Table[{{0.0000035, 0.0000001531}, {0.0000050, 0.0000001804}, {0.0000075, 0.0000002265},
{0.0000100, 0.0000002552}, {0.0000200, 0.0000003396}, {0.0000300, 0.0000003995}, {0.0000400, 0.0000004373},
{0.0000500, 0.0000003465}, {0.00035, 0.0000004732}, {0.00050, 0.0000005581}, {0.00075, 0.0000006615},
{0.00100, 0.0000007077}, {0.00200, 0.0000009137}, {0.00300, 0.000001059}, {0.00400, 0.000001180},
{0.00500, 0.000001334}, {0.007, 0.000001447}, {0.01, 0.000001718}, {0.015, 0.000002222},
{0.02, 0.000002956}, {0.0400, 0.000005583}, {0.0600, 0.000009437}, {0.0800, 0.00001209},
{0.100, 0.00001338}}];

q2 = Table[{{0.0000001531, Log[0.0000001531 * (1 - 0.0000035) / 0.0000035]},
    {0.0000001804, Log[0.0000001804 * (1 - 0.0000050) / 0.0000050]},
    {0.0000002265, Log[0.0000002265 * (1 - 0.0000075) / 0.0000075]},
{0.0000002552, Log[0.0000002552 * (1 - 0.0000100) / 0.0000100]},
    {0.0000003396, Log[0.0000003396 * (1 - 0.0000200) / 0.0000200]},
    {0.0000003995, Log[0.0000003995 * (1 - 0.0000300) / 0.0000300]},
    {0.0000004373, Log[0.0000004373 * (1 - 0.0000400) / 0.0000400]},
    {0.0000003465, Log[0.0000003465 * (1 - 0.0000500) / 0.0000500]},
    {0.0000004732, Log[0.0000004732 * (1 - 0.00035) / 0.00035]}, {0.0000005581, Log[0.0000005581 * (1 - 0.00050) / 0.00050]},
    {0.0000006615, Log[0.0000006615 * (1 - 0.00075) / 0.00075]},
{0.0000007077, Log[0.0000007077 * (1 - 0.00100) / 0.00100]}, {0.0000009137, Log[0.0000009137 * (1 - 0.00200) / 0.00200]},
    {0.000001059, Log[0.000001059 * (1 - 0.00300) / 0.00300]}, {0.000001180, Log[0.000001180 * (1 - 0.00400) / 0.00400]},
    {0.000001334, Log[0.000001334 * (1 - 0.00500) / 0.00500]}, {0.000001447, Log[0.000001447 * (1 - 0.007) / 0.007]},
    {0.000001718, Log[0.000001718 * (1 - 0.01) / 0.01]}, {0.000002222, Log[0.000002222 * (1 - 0.015) / 0.015]},
{0.000002956, Log[0.000002956 * (1 - 0.02) / 0.02]}, {0.000005583, Log[0.000005583 * (1 - .0400) / .0400]},
    {0.000009437, Log[0.000009437 * (1 - 0.0600) / 0.0600]}, {0.00001209, Log[0.00001209 * (1 - 0.0800) / 0.0800]},
    {0.00001338, Log[0.00001338 * (1 - 0.100) / 0.100]}}];

qq1 = ListPlot[q1, PlotRange -> {{0.0, 0.1}, {0, 0.00001550}}, AxesOrigin -> {0.0, 0},
AxesLabel -> {"xb", "xa"}, PlotStyle → {PointSize[0.1], Black}, PlotMarkers → {"●"}]

qq2 = ListPlot[q2, PlotRange -> {{0, 0.00001550}, {-10, -3}}, AxesOrigin -> {0.0, -10},
AxesLabel -> {"xa", "Log[xa(1-xb)/xb]  (Ono-Kondo)"}, PlotStyle → {PointSize[0.1], Black}, PlotMarkers → {"●"}]
```

```
q1 = Table[{{0.0000035, 0.00000002816}, {0.0000050, 0.00000003162}, {0.0000075, 0.00000003163},
{0.0000100, 0.00000003434}, {0.0000200, 0.00000003459}, {0.0000300, 0.00000003696}, {0.0000400, 0.00000003635},
{0.0000500, 0.00000004914} {0.00035, 0.00000003836}, {0.00050, 0.00000004422}, {0.00075, 0.00000004398},
{0.00100, 0.00000004157}, {0.00200, 0.00000004434}, {0.00300, 0.00000004346}, {0.00400, 0.00000004487},
{0.00500, 0.00000004441}, {0.007, 0.00000003547}, {0.01, 0.00000003516}, {0.015, 0.00000003384},
{0.02, 0.00000003933}, {0.0400, 0.00000003850}, {0.0600, 0.00000004020}, {0.0800, 0.00000003965},
{0.100, 0.00000004447}}];

q2 = Table[{{0.00000002816, Log[0.00000002816 * (1 - 0.0000035) / 0.0000035]},
    {0.00000003162, Log[0.00000003162 * (1 - 0.0000050) / 0.0000050]},
    {0.00000003163, Log[0.00000003163 * (1 - 0.0000075) / 0.0000075]},
{0.00000003434, Log[0.00000003434 * (1 - 0.0000100) / 0.0000100]},
    {0.00000003459, Log[0.00000003459 * (1 - 0.0000200) / 0.0000200]},
    {0.00000003696, Log[0.00000003696 * (1 - 0.0000300) / 0.0000300]},
    {0.00000003635, Log[0.00000003635 * (1 - 0.0000400) / 0.0000400]},
    {0.00000004914, Log[0.00000004914 * (1 - 0.0000500) / 0.0000500]},
    {0.00000003836, Log[0.00000003836 * (1 - 0.00035) / 0.00035]},
    {0.00000004422, Log[0.00000004422 * (1 - 0.00050) / 0.00050]},
    {0.00000004398, Log[0.00000004398 * (1 - 0.00075) / 0.00075]},
{0.00000004157, Log[0.00000004157 * (1 - 0.00100) / 0.00100]}, {0.00000004434, Log[0.00000004434 * (1 - 0.00200) / 0.00200]},
    {0.00000004346, Log[0.00000004346 * (1 - 0.00300) / 0.00300]},
    {0.00000004487, Log[0.00000004487 * (1 - 0.00400) / 0.00400]},
    {0.00000004441, Log[0.00000004441 * (1 - 0.00500) / 0.00500]},
    {0.00000003547, Log[0.00000003547 * (1 - 0.007) / 0.007]}, {0.00000003516, Log[0.00000003516 * (1 - 0.01) / 0.01]},
    {0.00000003384, Log[0.00000003384 * (1 - 0.015) / 0.015]},
{0.00000003933, Log[0.00000003933 * (1 - 0.02) / 0.02]}, {0.00000003850, Log[0.00000003850 * (1 - .0400) / .0400]},
    {0.00000004020, Log[0.00000004020 * (1 - 0.0600) / 0.0600]}, {0.00000003965, Log[0.00000003965 * (1 - 0.0800) / 0.0800]},
    {0.00000004447, Log[0.00000004447 * (1 - 0.100) / 0.100]}};

qq1 = ListPlot[q1, PlotRange -> {{0.0, 0.1}, {0, 0.00000005000}}, AxesOrigin -> {0.0, 0},
AxesLabel -> {"xb", "xa"}, PlotStyle → {PointSize[0.1], Black}, PlotMarkers → {"●"}]

qq2 = ListPlot[q2, PlotRange -> {{0.0, 0.00000005000}, {-15, -3}}, AxesOrigin -> {0.0, -5},
AxesLabel -> {"xa", "Log[xa(1-xb)/xb] (Ono-Kondo)"}, PlotStyle → {PointSize[0.1], Black}, PlotMarkers → {"●"}]
```

Bibliography

1. Calvert, J. G. “Glossary of atmospheric chemistry terms (Recommendations 1990)”. Pure and Applied Chemistry, 62.11, 2167-2219 (2009).

2. Cussler, E. L. “Diffusion: Mass Transfer in Fluid Systems (2nd ed.)”. New York: Cambridge University Press. 308–330 (1997). ISBN 978-0-521-45078-2

3. M. C. Desjonqueres; et al. “Concepts in surface physics (2nd ed.)”. New York: Springer-Verlag, (1996). ISBN 978-3-540-58622-7

4. Crini, edited by Grégorio; Badot, Pierre-Marie. “Sorption processes and pollution: conventional and non-conventional sorbents for pollutant removal from wastewaters”. Besançon: Presses universitaires de Franche-Comté. 43 (2010). ISBN 978-2-848-67304-4.

5. Lemaire, E.F. “Adsorption sélective et diffusion de paraffines linéaires et branchées en C6 sur la zéolithe ZSM-5: influence de la transition de phase monoclinique-orthorhombique du matériau poreux sur le processus d'adsorption”. Physique: Dijon (2004).

6. Oura, K.; Lifshits, V.G.; Saranin, A.A.; Zotov, A.V.; Katayama, M. “Surface Science, An Introduction”. Springer. (2003). ISBN 3-540-00545-5.

7. William Bleam, “Chapter 8 - Surface Chemistry and Adsorption, Soil and Environmental Chemistry (Second Edition)”. Academic Press 385-443 (2017). ISBN 978-0-128-04178-9.

8. Rouquerol, Françoise, J. Rouquerol, and K. S. W. Sing. “Adsorption by Powders and Porous Solids: Principles, Methodology, and Applications”. San Diego: Academic Press, 1999.

9. Brunauer, S., Emmett, P. H. & Teller, E. “Adsorption of gases in multimolecular layers”. J. Am. Chem. Soc. 60, 309–319 (1938).

10. Rouquerol, J.; et al. “Recommendations for the characterization of porous solids”. Pure Appl. Chem. 66, 1739–1758 (1994)

11. Thommes, M. et al. “Physisorption of gases, with special reference to the evaluation of surface area and pore size distribution (IUPAC Technical Report)”. Pure Appl. Chem. 87, (2015).

12. Hanaor, D.A.H., Ghadiri, M., Chrzanowski, W. & Gan, Y. “Scalable surface area characterization by electrokinetic analysis of complex anion adsorption”. Langmuir 30, 15143–15152 (2014).

13. Masel, Richard. “Principles of Adsorption and Reaction on Solid Surfaces”. Wiley Interscience. (1996): 240. ISBN 978-0-471-30392-3

14. Aranovich, G. L.; Donohue, M. D. “Surface compression in adsorption systems”. Colloids Surf. A 95, 187-188 (2001).

15. Rice, S. A., Gryko,J, Mohanty,U. “In Fluid Interfacial Phenomena”. Croxton, C. A., Ed.; John Wiley: New York. Section 6 (1986).

16. Rittner, F., Boddenberg, B., Bojan, M. J., Steele,W.A. “Adsortion of nitrogen on rutile (110): Monte Carlo computer simulations”. Langmuir. 15 1456 (1999).

17. D’Evelyn, M. P., Rice, S. A. Phys. Rev. Lett. 47, 1844 (1982); Discuss. Faraday Soc. 16, 71 (1982); J. Chem. Phys. 78, 5081 (1983); J. Chem. Phys. 78, 5225 (1983).

18. Heuberger, M.; Zach, M.; Spenser, N. D. “Density fluctuations under confinement: when is a fluid not a fluid?”. Science 292, 905 (2001).

19. Israelachvili, J.; Gourdon, D. “Putting liquids under molecular-scale confinement”. Science 292, 867 (2001).

20. Fairbrother, D. H.; Roberts, J. G.; Rizzi, S.; Somorjai, G. A. “Structure of monolayer and multilayer magnesium chloride films grown on Pd (111)”. Langmuir 13, 2090 (1997).

21. Karnaukhov, A. P. J. “Improvement of methods for surface area determinations” Colloid Interface Sci. 103, 311 (1985).

22. Aranovich, G. L. & Donohue, M. D. “Adsorption compression: An important new aspect of adsorption behavior and capillarity”. Langmuir 19, 2722–2735 (2003).

23. Aranovich, G. L., Sangwichien, C. & Donohue, M. D. “Intermolecular repulsions in adsorbed layers”. J. Colloid Interface Sci. 227, 553–560 (2000).

24. Lennard-Jones, J. E. "On the determination of molecular fields", Proc. R. Soc. Lond. A, 106 (738): 463–477 (1924).

25. Sangwichien, C., Aranovich, G. & Donohue, M. D. “Adsorption Compression Analysis for Supercritical Fluids using Ono-Kondo Model”. Ajche 11, 45–52 (2011).

26. Sumanatrakul, P., Abaza, S., Aranovich, G. L., Sangwichien, C. & Donohue, M. D. “Pattern of adsorption isotherms in Ono-Kondo coordinates”. J. Colloid Interface Sci. 368, 427–433 (2012).

27. Singh, Jayant K., and Verma, Nishith, eds. “Aqueous Phase Adsorption: Theory, Simulations, and Experiments”. Milton: CRC Press LLC, 2018.

28. Brooks, Steve, Gelman, Andrew, and Jones, Galin, eds. “Handbook of Markov Chain Monte Carlo”. London: CRC Press LLC, 2011.

29. Nicholas, M., Arianna, W. R., Marshall, N. R., Augusta, H. T. & Edward, T. “Equation of State Calculations by Fast Computing Machines”. J. Chem. Phys. 21, 1087–1092 (1953).

30. Hastings, A. W. K. “Monte Carlo Sampling Methods Using Markov Chains and Their Applications” Published by: Biometrika Trust Stable URL: http://www.jstor.org/stable/2334940. Biometrika 57, 97–109 (2008).

31. Abaza, S., Aranovich, G. L. & Donohue, M. D. “Adsorption compression in surface layers”. Mol. Phys. 110, 1289–1298 (2012).

32. Limtrakul, J., Khongpracha, P., Jungsuttiwong, S. & Truong, T. N. “Adsorption of carbon monoxide in H-ZSM-5 and Li-ZSM-5 zeolites: An embedded ab initio cluster study”. J. Mol. Catal. A Chem. 153, 155–163 (2000).

33. Szanyi, J. & Paffett, M. T. “The Adsorption of NO and Reaction of NO with O2 on H-, NaH-, CuH-, and Cu-ZSM-5: An in Situ FTIR Investigation”. J. Catal. 232–245 (1996). doi:10.1039/b306585e

34. Sethia, G. et al. “Equilibrium and dynamic adsorption of carbon monoxide and nitrogen on ZSM-5 with different SiO2/Al2O3ratio”. Sep. Sci. Technol. 45, 413–420 (2010).

35. Shirazi, L., Jamshidi, E. & Ghasemi, M. R. “The effect of Si/Al ratio of ZSM-5 zeolite on its morphology, acidity and crystal size”. Cryst. Res. Technol. 43, 1300–1306 (2008).

Curriculum Vitae

Yutian Qian was born on July 31st, 1995 in Shanghai, China, the son of Hong Qian and Ping Ji. Yutian spent most of his youth life with his grandma, Xiaoyuan Peng, who has been mentoring and caring Yutian for all her life. Yutian came to United States and joined his uncle's family after finishing his second-year study in Shanghai Yan'An High School. He attended Shoreline Community College in Washington state, graduated with honor, and transferred to University of Washington, Seattle. With his passion in chemistry and engineering, Yutian joined the Department of Chemical Engineering and made his mind to continue his study in Chemical Engineering after graduation.

After one gap year working as a software tester, Yutian applied for graduate school and got accepted to Johns Hopkins University. Yutian joined Dr. Donohue's group to work on exploring the characteristics of adsorption compression, a phenomenon that has a great potential to improve the performance of catalytic reaction. Under Dr. Donohue and Dr. Aranovich's guidance and supervision, Yutian finished his Masters studies in May 2019 and is going to attend the graduate school at Texas A&M University as a Chemical Engineering Ph.D student. Yutian has a long-term goal to use his chemical engineering skills learnt from the lab as well as from the classroom to secure a position in the industry.